Dalton Transactions

ROYAL SOCIETY OF CHEMISTRY

FRONTIER

View Article Online
View Journal | View Issue

Cite this: *Dalton Trans.*, 2025, **54**, 2224

Surface decorated metal carbonyl clusters: bridging organometallic molecular clusters and atomically precise ligated nanoclusters

Cristiana Cesari, Cristina Femoni, Francesca Forti, Maria Carmela Iapalucci, Giorgia Scorzoni and Stefano Zacchini *

In this Frontier Article, the work carried out within our research group in Bologna in the field of surface decorated metal carbonyl clusters will be outlined and put in a more general context. After a short Introduction, clusters composed of a metal carbonyl core decorated on the surface by metal–ligand fragments will be analyzed. Both metal–ligand fragments behaving as Lewis acids and Lewis bases will be considered. Then, the focus will be moved to clusters composed of a naked metal core decorated and stabilized on the surface by metal-carbonyl fragments. The structure and bonding (where theoretical studies are available) of such surface decorated metal carbonyl clusters will be presented, and compared to atomically precise ligated nanoclusters.

Received 22nd November 2024,
Accepted 7th January 2025

DOI: 10.1039/d4dt03266g

rsc.li/dalton

1. Introduction

According to F. A. Cotton, metal atom clusters are "...compounds containing a finite group of metal atoms which are held together entirely, mainly, or at least to a significant extent, by bonds directly between the metal atoms even

Dipartimento di Chimica Industriale "Toso Montanari", Università di Bologna, Via P. Gobetti 85, 40129 Bologna, Italy. E-mail: stefano.zacchini@unibo.it

Cristiana Cesari

Cristiana Cesari: Cristiana Cesari received the Master Degree in Industrial Chemistry from the University of Bologna in 2012, and in 2016 was awarded a Ph.D. in Chemistry from the University of Bologna. Her doctoral research was focused on the synthesis, characterization and catalytic application of ruthenium N-heterocyclic carbene complexes. After a post-doctoral fellowship in Bologna focused on the study of the transformation process of ethanol to butanol via *both homogeneous and heterogeneous catalysis, in 2019, she became a researcher in the field of General and Inorganic Chemistry at the University of Bologna. Her research activityis aimed at the synthesis of molecular organometallic compounds containing low valent transition metals stabilized by ligands, focusing on the study of metal carbonyl cluster as atomically defined nanomaterials for electrochemical applications and as precursors of nanostructured catalytic systems*

Cristina Femoni

Cristina Femoni: Cristina Femoni received her Degree cum laude *in Industrial Chemistry from the University of Bologna working on an experimental thesis under the supervision of Prof. G. Longoni. After a brief industrial working experience in France, in 1999 she was awarded a PhD in Chemical Sciences from the University of Bologna. Since 2022 she is full professor of General and Inorganic Chemistry. Her main scientific interests and expertise lie in the synthesis and characterization, also by single-crystal X-ray diffraction, of high-nuclearity transition metal clusters stabilized by carbonyl ligands, also referred to as atomically-precise ligand-stabilized nanoclusters, and their application in catalysis and nanoscience. She has been elected President of the European Chemistry Thematic Network (ECTN).*

though some non-metal atoms may be associated intimately with the cluster...".[1] There are nowadays several categories of compounds that fall within Cotton's definition, including clusters composed of many types of transition and main group metals, in low to high oxidation states, and stabilized by a large variety of inorganic and organic ligands.[2–8] Metal carbonyl clusters (MCC) represent one of the most important category of organometallic and low-valent molecular metal clusters.[9–24] The chemistry of MCCs is well developed, and they played a fundamental role for Cotton's definition of metal clusters.

A similar consideration applies to gold-phosphine clusters, another category of low valent metal clusters, that was developed almost contemporarily to MCCs.[25] Indeed, following the pioneering work of Malatesta and Naldini in the 1960s,[26–29] several gold-phosphine clusters were characterized between 1970 and 2000. Since the turn of the century the range of gold cluster compounds has been greatly extended by the study of organothiolato-gold clusters. Indeed, molecular gold clusters and nanoclusters protected by thiolate ligands represent a very important field of research in modern inorganic chemistry and nanochemsitry.[30–35] This field has been further expanded, including other organic ligands, as well as other metals, and alloy nanoclusters.[36–38] Molecular clusters find nowadays several applications, including catalysis, electrocatalysis, material chemistry, sensing, medicine, biology.[39–43]

As in the early days of metal cluster chemistry, single crystal X-ray diffraction (SC-XRD) represents the most important technique for the complete characterization of the structures of metal clusters. The SC-XRD analysis of $[Au_{102}(p\text{-MBA})_{44}]$ (*p*-MBA = *p*-mercaptobenzoic acid) represented somehow a milestone and showed some interesting features.[44] First of all, its metal core does not possess a *ccp* structure, as found in larger Au nanoparticles and bulk Au, but is based on an icosahedral structure. Moreover, the thiolato ligands are not innocent, but strongly interact with surface Au atoms, forming $[Au_n(SR)_{n+1}]^-$ staple motives which decorate the surface of the cluster. Similar structures have been found for several other thiolate protected Au nanoclusters, and linear RS–Au–SR staple motives are nowadays a common features in cluster chemistry.[45]

Different models have been developed for the interpretation of bonding in molecular metal clusters. In the case of low valent metal clusters, including MCCs, the most noticeable models for their electron counting are the effective atomic number (EAN) rule, Wade's rules, the polyhedral skeletal electron pair theory (PSEPT), and topological electron counting (TEC).[25,46] Regarding thiolate protected gold nanoclusters, and related molecular nanoclusters, their bonding has been usually rationalized based on the superatom model.[47–49] Recently, the superatom model has been successfully applied also to some MCCs, in particular Pt MCCs decorated on the surface by Cd-halide or Au-phosphine fragments, as well as Au, Ag and Cu clusters stabilized on the surface by Fe–CO, Ni–CO, Nb–CO or Ta–CO fragments.[50–53] These are representative examples of the two main categories of surface decorated MCCs, that is: (1) clusters composed of a metal carbonyl core decorated on the surface by ML fragments; (2) clusters composed of a naked metal core decorated and stabilized on the surface by metal-carbonyl fragments. These theoretical studies suggest some analogies between surface decorated MCCs and atomically precise ligated nanoclusters. Further analogies become evident when their structures are analyzed. Indeed, the metal–ligand and metal-CO fragments decorating the surfaces of such MCCs are somehow reminiscent of the staple motives found in atomically precise ligated nanoclusters. One of the aim of this Frontier Article is to stimulate further theoretical studies in order to investigate the possibility of extending the applicability of the superatom model to other MCCs and, at the same time, to compare it with other theoretical models. This might lead to a general unified approach for the interpretation of the different categories of molecular ligated metal clusters.

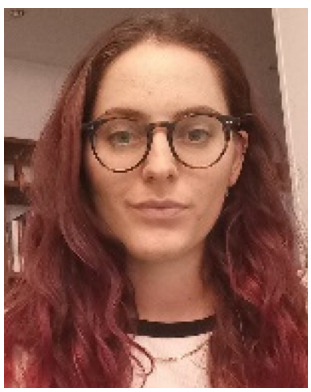

Francesca Forti

Francesca Forti: Francesca Forti received the Master Degree in Industrial Chemistry from the University of Bologna in 2021, and the same year started her Ph.D. in Chemistry at the University of Bologna. Her doctoral research is focused on the synthesis and characterization of new heterometallic carbonyl clusters and their application in catalytic reactions. In 2023 she joined Professor Nordlander's group in University of Lund for a visiting period to conduct synthesis and characterization of Os–Rh carbonyl clusters bearing chiral phosphines, exploited as asymmetric catalysts.

Maria Carmela Iapalucci

Maria Carmela Iapalucci: Maria Carmela Iapalucci received the Degree in Industrial Chemistry from the University of Bologna in 1987 with an experimental thesis under the supervision of Prof. G. Rosini. In 1992, she received her PhD in Chemical Sciences from the University of Bologna, working on the synthesis and characterization of iron and nickel carbonyl clusters containing group XIII and XV heteroatoms, under the supervision of Prof. G. Longoni. Since 2001 she is associate professor of General and Inorganic Chemistry at the University of Bologna.

Our group has worked in the field of surface decorated MCCs over the last 15 years, and the most noticeable results are summarized in this Frontier Article. After this short Introduction, section 2 will be dedicated to clusters composed of a metal carbonyl core decorated on the surface by ML fragments. This will be further divided based on the fact that the surface ML fragments may act as Lewis acids (section 2.1) or Lewis bases (section 2.2). Then, section 3 will be focused on clusters composed of a naked metal core decorated and stabilized on the surface by metal-carbonyl fragments. For each category of surface decorated MCCs, the most representative examples taken from our work will be presented together with the most relevant compounds published in the literature. The structure and bonding (where theoretical studies are available) of such surface decorated MCCs will be presented, and compared to atomically precise ligated nanoclusters. The applications of MCCs in catalysis and electrocatalysis have been recently reviewed.[9,13] A short perspective on the potential and prospects of MCCs in practical applications will be reported in the Conclusions. All the structures reported in the following figures have been determined by SC-XRD.

2. Metal carbonyl core decorated on the surface by metal–ligand fragments

2.1. Metal–ligand fragments as Lewis acids

There are several examples of MCCs decorated on the surface by metal–ligand fragments of general formula $\{M_xL_y\}^z$ (x, y = 1, 2, 3...; z = 0, positive or negative; M = transition or p-block metal; L = neutral or anionic ligand). These fragments may act as Lewis acids or Lewis bases. The former behaviour will be discussed in this section, the latter in section 2.2.

Cationic $[Au(PR_3)]^+$ groups are the archetype of metal–ligand fragments that can coordinate as Lewis acids on the surface of MCCs. Indeed, several examples of MCCs decorated by $[Au(PR_3)]^+$ fragments are known, and this topic has been recently reviewed.[15] $[Au(PR_3)]^+$ fragments possess 12-electrons, and the d^{10} Au(I) centre may accept electron density from the MCC surface on its empty orbitals (s, p or hybridized orbitals). It must be remarked that coordination of a 12 electron fragment does not alter the electron count of a MCC. This concept can be extended to other 12 electron ML fragments, including group 12 metals $[ML]^{2+}$ and $[MX]^+$ fragments (M = Zn, Cd, Hg; L = neutral ligand; X = anionic ligand), group 11 metals $[ML]^+$ and [MX] fragments (M = Cu, Ag, Au), group 10 metals [ML] fragments (M = Ni, Pd, Pt), and group 9 metals $[ML_2]^+$ fragments (M = Co, Rh, Ir).

Earlier interest was due to the isolobal analogy between $[Au(PR_3)]^+$ and H^+.[54–57] As soon as structures of MCCs containing two or more $[Au(PR_3)]^+$ fragments were discovered, it was realized that Au(I) centres could reciprocally attract due to aurophilic interactions.[58–63] Indeed, peraurated MCCs revealed to be suitable platforms to study aurophilicity. This generates $[\{Au(PR_3)\}_n]^{n+}$ fragments, which are strictly related to the Au-thiolate staple motives found in molecular Au nanoclusters.

Since aurophilic interactions are rather weak, MCCs decorated by $[Au(PR_3)]^+$ fragments may show fluxionality and/or isomerism (Fig. 1 and 2).[64–67]

Moreover, coordination of $[Au(PR_3)]^+$ fragments may favour the stabilisation and isolation of MCCs, that otherwise cannot be observed as free species.[68] For instance, perauration allows the isolation of Ni carbide MCCs such as $[Ni_6(C)(CO)_9(AuPPh_3)_4]^{2-}$ and $[Ni_6(C)(CO)_8(AuPPh_3)_8]^{2+}$, containing a carbide atom within an octahedral Ni_6 cages (Fig. 3).[69,70]

The reaction of $[Pt_{19}(CO)_{22}]^{4-}$ with CO affords a purported $[Pt_{19}(CO)_{22}]^{4-}$ cluster, which has never been isolated, since the

Giorgia Scorzoni

Giorgia Scorzoni: Giorgia Scorzoni received the Master Degree in Industrial Chemistry from the University of Bologna in 2022. After spending one year as a research fellow in the field of Inorganic Chemistry, she started her Ph.D. in Industrial Chemistry at the University of Bologna. Her research activities focus on synthesis and characterization of new rhodium carbonyl clusters differentially substituted.

Stefano Zacchini

Stefano Zacchini: Stefano Zacchini received the Degree in Industrial Chemistry from the University of Bologna in 1996, working on an experimental Thesis under the supervision of Prof. G. Longoni. In 2001, he received his PhD in Chemistry from the University of Liverpool under the direction of Prof. B. T. Heaton. After a post-doctoral fellowship in Liverpool, he joined the University of Bologna in 2002 as research associate. In 2010, he has been appointed Associate Professor of General and Inorganic Chemistry at the University of Bologna and in 2017 he became full Professor. His research program focuses on the chemistry of metal carbonyl clusters and their applications in nanotechonolgy and nanosciences, molecular electronics and catalysis.

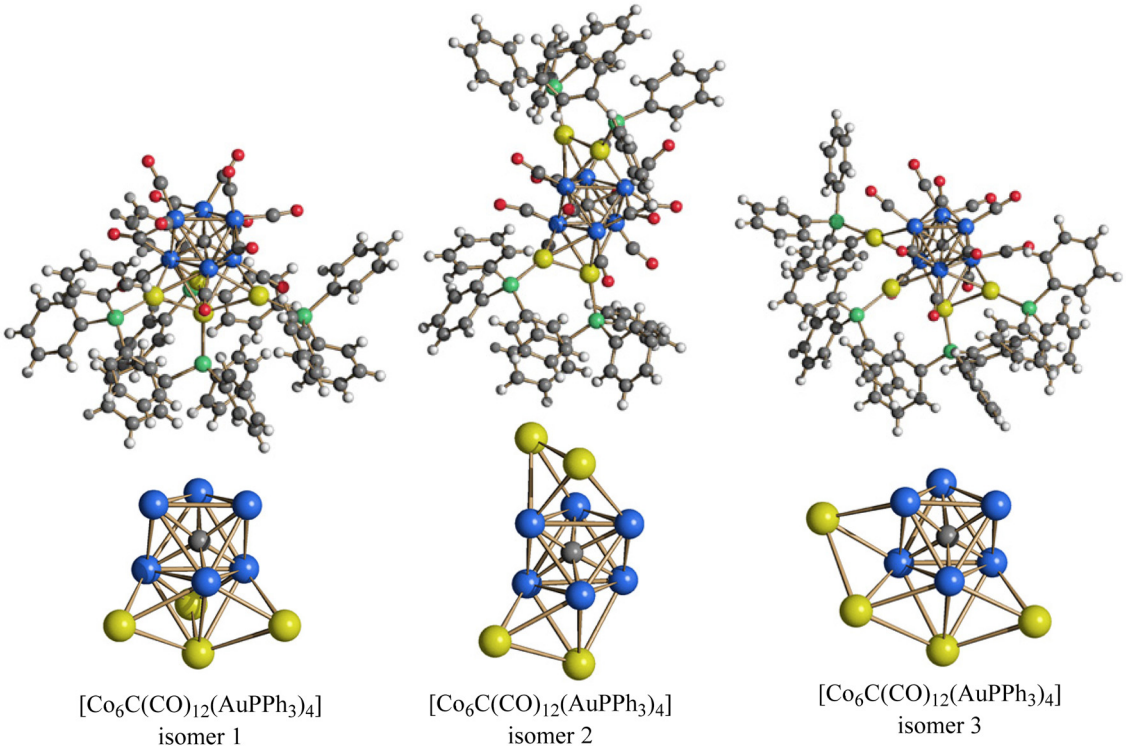

Fig. 1 Three isomers of $[Co_6C(CO)_{12}(AuPPh_3)_4]$ are formed upon crystallization, as found in the crystals of $[Co_6C(CO)_{12}(AuPPh_3)_4]$, $[Co_6C(CO)_{12}(AuPPh_3)_4]\cdot THF$ and $[Co_6C(CO)_{12}(AuPPh_3)_4]\cdot 4THF$ (blue, Co; yellow, Au; green, P; red, O; grey, C; white, H). Adapted with permission from ref. 64 Copyright 2014 American Chemical Society.

reaction is reversed upon crystallization. Nonetheless, it has been possible to trap this elusive $[Pt_{19}(CO)_{24}]^{4-}$ species by addition of 3–4 $[Au(PPh_3)]^+$ fragments, affording the surface decorated clusters $[Pt_{19}(CO)_{24}(AuPPh_3)_3]^-$ and $[Pt_{19}(CO)_{24}(AuPPh_3)_4]$ (Fig. 4).[71] Interestingly, $[Pt_{19}(CO)_{24}(AuPPh_3)_3]^-$ is decorated by three isolated $[Au(PPh_3)]^+$ fragments, whereas $[Pt_{19}(CO)_{24}(AuPPh_3)_4]$ contains two $[\{Au(PPh_3)\}_2]^{2+}$ fragments showing one aurophilic interaction each.

The cluster $[Os_{10}C(CO)_{24}Au(AuPCy_3)_3]$ is rather peculiar, since it may be viewed as a $[Os_{10}C(CO)_{24}]$ tetrahedron of frequency two decorated on one edge by a $[Au_4(PCy_3)_3]$ tetrahedral unit (Fig. 5).[72] This is a rare case of a MCC decorated by an Au-phosphine cluster.

The concepts developed for $[Au(PR_3)]^+$ fragments can be applied to related fragments obtained using other monodenate or polydentate ligands, or replacing Au(I) with other coinage metal ions, that is, Cu(I) and Ag(I). Several examples of MCCs decorated by $[ML]^+$ (M = Cu, Ag, Au; L = neutral ligand) or MX (M = Cu, Ag, Au; X = anionic ligand) fragments are, indeed, known.

NHC ligands have recently attracted a large interest in catalysis, coordination and organometallic chemistry. Examples of MCCs decorated by $[M(NHC)]^+$ (M = Cu, Ag, Au) fragments have been, also, reported, even though their nuclearity is usually rather limited.[73–82] The largest species reported so far are $[Pt_6(CO)_{12}(AgIPr)_2]$ and $[Pt_9(CO)_{18}(AgIPr)_2]$ [IPr = $C_3N_2H_2(C_6H_3{}^iPr_2)_2$] obtained from the reactions of Chini clusters $[Pt_6(CO)_{12}]^{2-}$ and $[Pt_9(CO)_{18}]^{2-}$, respectively, with Ag(IPr)Cl (Fig. 6).[83] In these cases, the two $[AgIPr]^+$ fragments cap the external triangular faces of the Chini clusters with retention of their prismatic structures.

Clusters with higher nuclearities have been obtained upon capping Ni carbide MCCs with CuCl and $[Cu(MeCN)]^+$ fragments (Fig. 7), as in the case of $[HNi_{42}C_8(CO)_{44}(CuCl)]^{7-}$ and $[H_2Ni_{29+x}(CO)_{33+x}\{Cu(MeCN)\}_2]^{4-}$ (x = 0, 1).[84–86] The two $[Cu(MeCN)]^+$ fragments in the latter cluster may be formally replaced with isoelectronic $[CdX]^+$ (X = Cl, Br, I) or Ni(CO) fragments, affording $[H_{6-n}Ni_{30}C_4(CO)_{34}(CdX)_2]^{n-}$ (n = 3–6), $[H_{7-n}Ni_{32}C_4(CO)_{36}(CdX)]^{n-}$ (n = 5–7), and $[H_{6-n}Ni_{34+x}C_4(CO)_{38+x}]^{n-}$ (n = 5, 6; x = 0, 1).[87,88] All these clusters are based on the same tetracarbide $Ni_{30}C_4$ core. Similarly, replacing the CuCl fragment of $[HNi_{42}C_8(CO)_{44}(CuCl)]^{7-}$ with $[CdX]^+$ (X = Cl, Br) or Ni(CO) fragments results in related $[Ni_{42+x}C_8(CO)_{44+x}(CdCl)]^{7-}$ (x = 0, 1), $[HNi_{42+x}C_8(CO)_{44+x}(CdBr)]^{6-}$ (x = 0, 1), $[HNi_{43}C_8(CO)_{45}]^{7-}$, $[HNi_{44}C_8(CO)_{46}]^{7-}$, $[H_2Ni_{43}C_8(CO)_{45}]^{6-}$, and $[H_2Ni_{44}C_8(CO)_{46}]^{6-}$.[84,85,89] All these clusters possess a common $Ni_{42}C_8$ core differently capped by miscellaneous [CuCl], $[CdX]^+$, and [Ni(CO)] fragments and may be viewed as borderline compounds between molecular and quasi-molecular clusters. It must be remarked that from a synthetic point of view, clusters containing Cu and Cd are usually obtained from the reactions of preformed Ni carbide MCCs such as $[Ni_9C(CO)_{17}]^{2-}$, $[Ni_{10}(C_2)(CO)_{16}]^{2-}$, $[Ni_{16}(C_2)_2(CO)_{23}]^{4-}$,

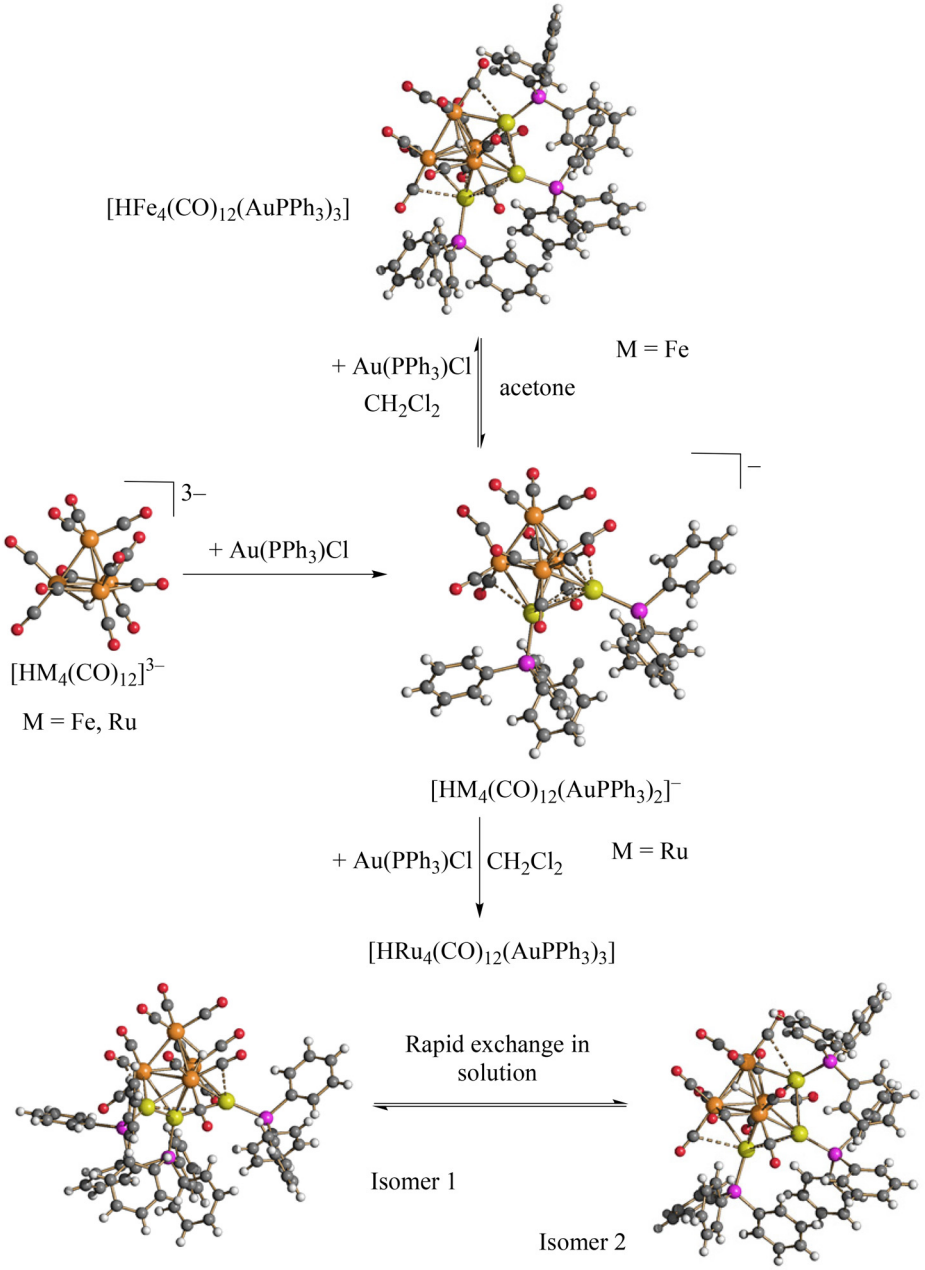

Fig. 2 Reactions of $[HM_4(CO)_{12}]^{3-}$ (M = Fe, Ru) with increasing amounts of $Au(PPh_3)Cl$ result in the formation of $[HM_4(CO)_{12}(AuPPh_3)_2]^-$ and $[HM_4(CO)_{12}(AuPPh_3)_3]$. Anionic Fe and Ru clusters are isostructural, whereas noticeable differences are detected for the neutral clusters. $[HFe_4(CO)_{12}(AuPPh_3)_3]$ displays the unique hydride within the tetrahedral Fe_4 cavity, and its formation is reversed in polar solvents such as acetone. $[HRu_4(CO)_{12}(AuPPh_3)_3]$ exists as two isomers in rapid exchange in solution, both displaying the hydride ligand on the surface of the cluster (orange, Fe or Ru; yellow, Au; purple, P; red, O; grey, C; white, H).

and $[Ni_{38}C_6(CO)_{42}]^{6-}$, with CuCl, $[Cu(MeCN)_4][BF_4]$ and CdX_2. Homometallic Ni species are obtained from the chemical oxidation of the same carbide species. Thus, since Cu(I) and Cd(II) salts may act also as oxidants, sometimes mixtures of species are obtained, that contain a variable amount of $[CdX]^+$/Ni(CO), CuCl/Ni(CO) or $[Cu(MeCN)]^+$/Ni(CO) fragments.

Capping a cluster with Ni(CO) fragments is very common and, indeed, several Ni MCCs displaying the same metal core decorated by a variable amount of Ni(CO) fragments are known (Fig. 8).[84,85,89–91] Even though apparently different, it must be remarked that both in the cases of Ni MCCs and Au thiolated nanoclusters, capping fragments and metal core are based on the same metals, that is, Ni in the case of Ni MCCs decorated by Ni(CO) fragments, Au in the case of Au nanoclusters with Au–SR staple motives.

As an alternative to Ni(CO), MCCs may also be decorated by $M(PR_3)$ or M(NHC) (M = Ni, Pd, Pt) fragments (Fig. 9).[92–96]

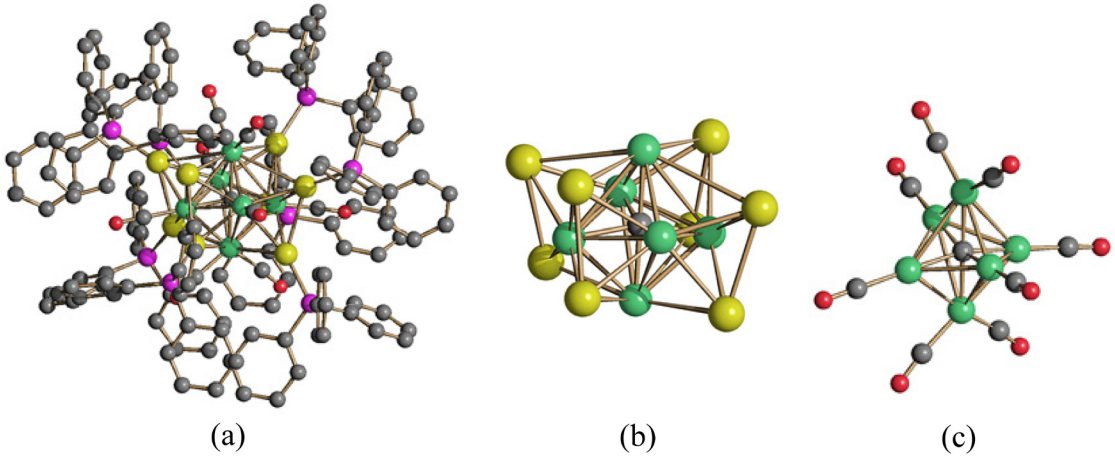

Fig. 3 Perauration of Ni-carbide MCCs results in the encapsulation of the carbide within an octahedral Ni_6 cage. Usually carbides are present within larger Ni cages, such as capped trigonal prismatic or square-antiprismatic. Molecular structure of (a) $[Ni_6(C)(CO)_8(AuPPh_3)_8]^{2+}$, (b) its $Ni_6(C)Au_8$ cage, and (c) its $[Ni_6(C)(CO)_8]^{6-}$ core (green, Ni; yellow, Au; purple, P; red, O; grey, C; H-atoms have been omitted for clarity). Surface decoration with $[Au(PR_3)]^+$ fragments results in the stabilization in the otherwise unknown $[Ni_6(C)(CO)_8]^{6-}$ cluster. Adapted from ref. 70 with permission from The Royal Society of Chemistry.

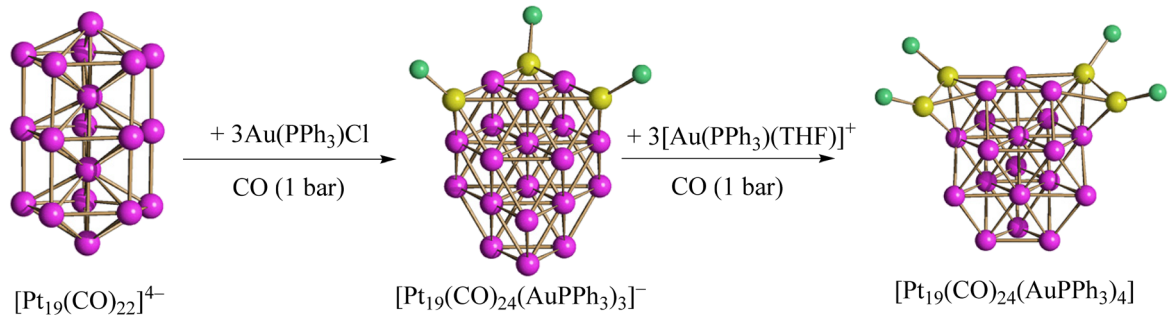

Fig. 4 The elusive $[Pt_{19}(CO)_{24}]^{4-}$ species has been trapped upon reaction of $[Pt_{19}(CO)_{22}]^{4-}$ with three moles of $Au(PPh_3)Cl$ under CO atmosphere. The resulting $[Pt_{19}(CO)_{24}(AuPPh_3)_3]^-$ monoanion further reacts with $[Au(PPh_3)(THF)]^+$ affording neutral $[Pt_{19}(CO)_{24}(AuPPh_3)_4]$. The homoleptic precursor $[Pt_{19}(CO)_{24}]^{4-}$ possesses a centered pentagonal prismatic structure, whereas the three- and tetra-aurated clusters display a compact *ccp* metal core (purple, Pt; yellow, Au; green, P; CO ligands and Ph-groups have been omitted for clarity).

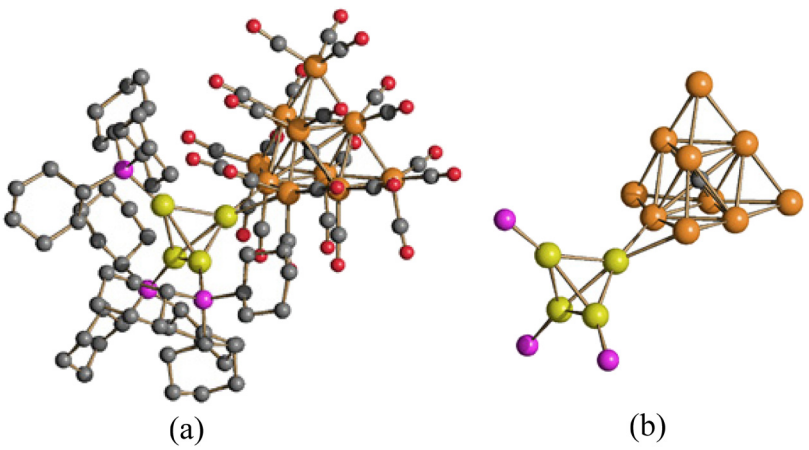

Fig. 5 A rare example of the MCCs decorated by an Au-phosphine cluster. (a) Molecular structure of $[Os_{10}C(CO)_{24}Au(AuPCy_3)_3]$, and (b) its $Os_{10}CAu_4P_3$ cage (orange, Os; yellow, Au; purple, P; red, O; grey, C). Hydrogen atoms have been omitted for clarity.

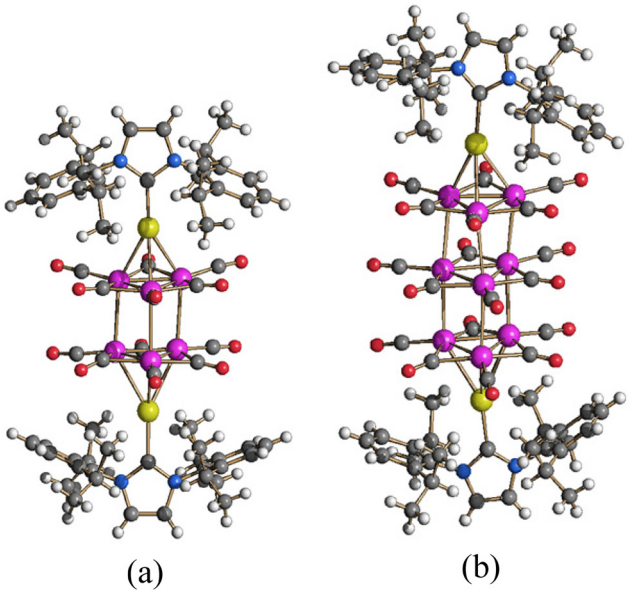

Fig. 6 MCCs decorated by $[M(NHC)]^+$ (M = Cu, Ag, Au) fragments. The molecular structure of (a) $[Pt_6(CO)_{12}(AgIPr)_2]$ and (b) $[Pt_9(CO)_{18}(AgIPr)_2]$ (purple, Pt; yellow, Ag; blue, N; red, O; grey, C; white, H). Adapted with permission from ref. 83 Copyright 2017 American Chemical Society.

Some impressive examples of MCCs decorated by $Ni(PR_3)$ and $Pd(PR_3)$ fragments are the homo and heterometallic Pd CO/PR_3-ligated clusters described by Dahl and Mednikov (Fig. 10).[12,97,98]

Group 9 metal fragments of the type $[ML_2]^+$ (M = Rh, Ir; L = neutral ligand) are isoelectronic to those described above and, thus, may be used in order to decorate MCCs. Nonetheless, very few examples are known.[99,100]

As shown above, some MCCs decorated by $[CdX]^+$ fragments have been reported, and the literature may be extended to related $[ZnX]^+$ and $[HgX]^+$ fragments. Cd(II) is rather versatile for this purpose, and other Cd-based fragments may be found, that is, CdX_2, $[Cd_2Cl_3]^+$ and $[Cd_5(\mu\text{-}Br)_5Br_{5-x}(solvent)_x]^{x+}$.[101–105]

Thermal decomposition in dfm at 120 °C of Chini clusters $[Pt_{3n}(CO)_{6n}]^{2-}$ (n = 2–6) in the presence of $CdBr_2{\cdot}H_2O$ under different experimental conditions selectively afford the surface decorated Pt–Cd nanoclusters $[Pt_{13}(CO)_{12}\{Cd_5(\mu\text{-}Br)_5Br_2(dmf)_3\}_2]^{2-}$, $[Pt_{19}(CO)_{17}\{Cd_5(\mu\text{-}Br)_5Br_3(Me_2CO)_2\}\{Cd_5(\mu\text{-}Br)_5Br(Me_2CO)_4\}]^{2-}$, and $[H_2Pt_{26}(CO)_{20}(CdBr)_{12}]^{8-}$.[106,107]

$[Pt_{13}(CO)_{12}\{Cd_5(\mu\text{-}Br)_5Br_2(dmf)_3\}_2]^{2-}$ is composed of a $Pt_{13}(CO)_{12}$ core decorated by two $\{Cd_5(\mu\text{-}Br)_5Br_2(dmf)_3\}$ rings (Fig. 11). Its electron count may be justified adopting either an ionic or covalent (radical) model. In the ionic model, the oxi-

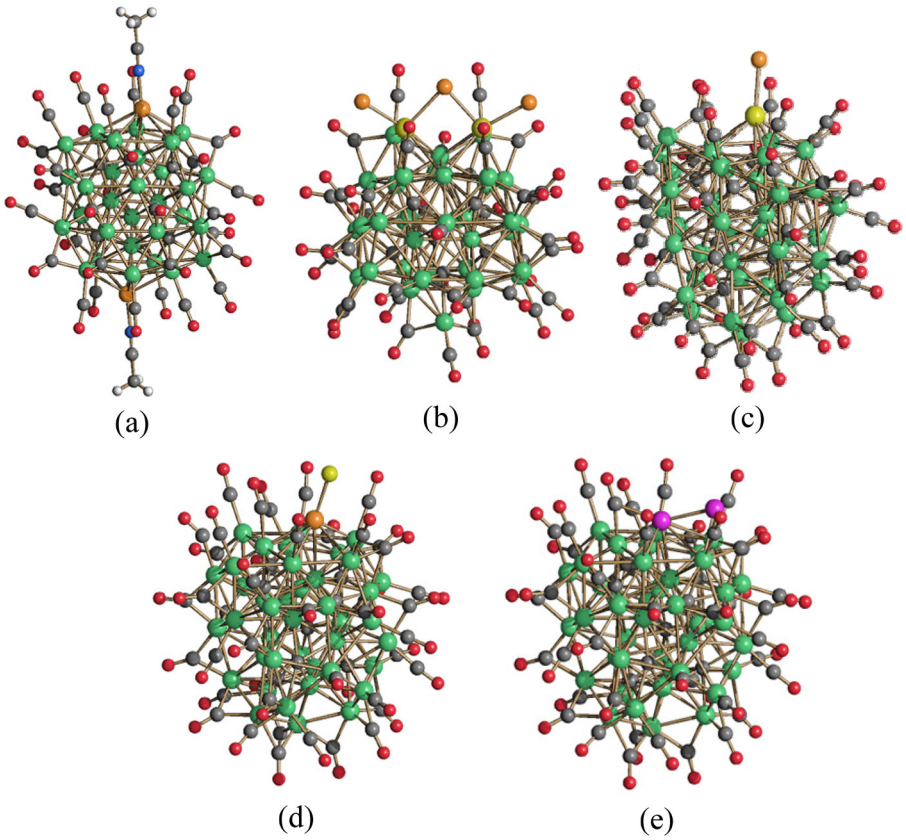

Fig. 7 Ni-carbide MCCs decorated by Cu and Cd-based fragments: (a) $[H_2Ni_{30}C_4(CO)_{34}\{Cu(MeCN)\}_2]^{4-}$ (green, Ni; orange, Cu; grey, C; red, O; blue, N; white, H); (b) $[Ni_{36}C_8(CO)_{36}(Cd_2Cl_3)]^{5-}$, (c) $[Ni_{42+x}C_8(CO)_{44+x}(CdCl)]^{7-}$ (x = 0.19) (green, Ni; yellow, Cd; orange, Cl; grey, C; red, O); (d) $[HNi_{42}C_8(CO)_{44}(CuCl)]^{7-}$ and (e) $[HNi_{43+x}C_8(CO)_{45+x}]^{7-}$ (two CO ligands with partial occupancy factors have not been located) (green, Ni; purple, Ni with partial occupancy factor; orange Cu; yellow, Cl; grey, C; red, O). Hydride ligands have not been located by SC-XRD. Adapted from ref. 84 and 85 with permission from Springer and Elsevier.

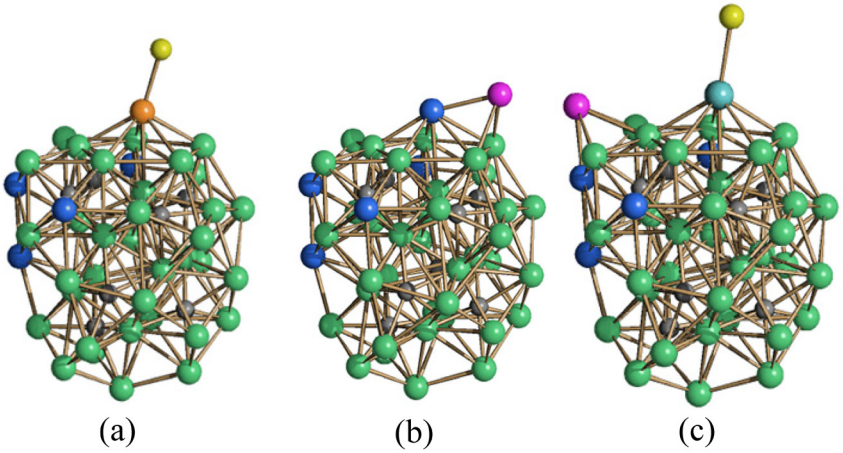

Fig. 8 Different Ni(CO) capping modes found in the $[HNi_{42}C_8(CO)_{44}(CuCl)]^{7-}$, $[HNi_{43+x}C_8(CO)_{45+x}]^{7-}$, $[H_2Ni_{43+x}C_8(CO)_{45+x}]^{6-}$, $[Ni_{42+x}C_8(CO)_{44+x}(CdCl)]^{7-}$ and $[HNi_{42+x}C_8(CO)_{44+x}(CdBr)]^{6-}$ clusters. (a) Uncapped $Ni_{42}C_8(CuCl)$ core; (b) mono-capped $Ni_{44}C_8$ core; (c) mono-capped $Ni_{43}C_8(CdX)$ core (green, Ni; grey, C; blue, Ni not bonded to carbide; purple, Ni with partial occupancy factor; orange, Cu; cyan, Cd; yellow, Cl or Br). Hydride ligands have not been located by SC-XRD. Adapted from ref. 84 with permission from Springer.

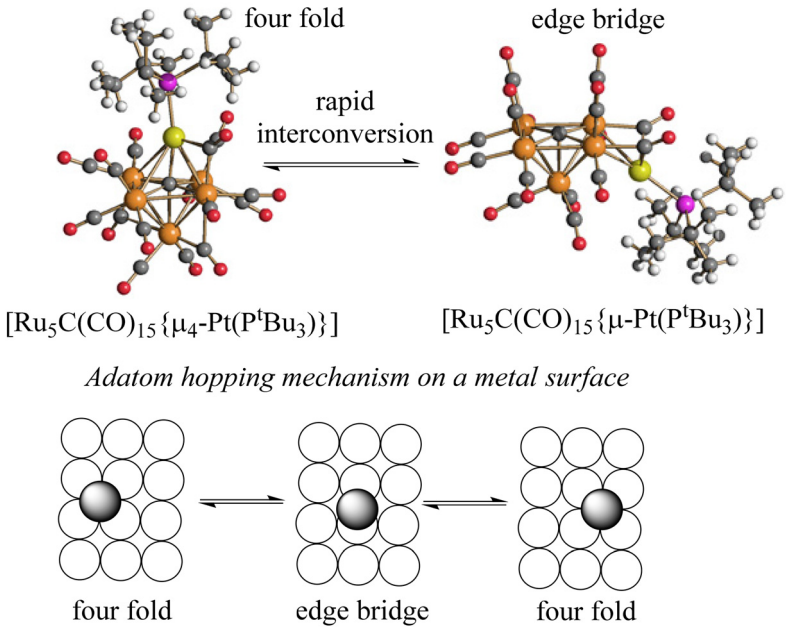

Fig. 9 (Top) Molecular structures of the two isomers $[Ru_5C(CO)_{15}\{\mu_4\text{-}Pt(P^tBu_3)\}]$ and $[Ru_5C(CO)_{15}\{\mu\text{-}Pt(P^tBu_3)\}]$ (orange, Ru; yellow, Pt; green, P; red, O; grey, C; white, H). The two isomers rapidly interconvert in solution, mimicking the shift of a metal atom from a 4-fold to a 2-fold bonding site and back on a metal surface during the hopping process. (Bottom) A schematic representation of the adatom hopping mechanism on a metal surface. Empty circles represent the metal surface; the shaded circle represent the atom that moves. Adapted with permission from ref. 92 Copyright 2003 American Chemical Society.

dation states of Cd and Br are assumed to be +2 and −1, respectively, and the cluster may be partitioned into two cationic $[\{Cd_5(\mu\text{-}Br)_5Br_2(dmf)_3\}]^{3+}$ rings and one $[Pt_{13}(CO)_{12}]^{8-}$ anionic core. The two rings act as Lewis acids *via* the Cd(II) centers, and overall $[Pt_{13}(CO)_{12}]^{8-}$ displays 162 cluster valence electrons (CVE) [13(Pt) × 10 + 12(CO) × 2 + 8(negative charge)]. In the covalent model, each $\{Cd_5(\mu\text{-}Br)_5Br_2(dmf)_3\}$ ring is assumed as neutral, and binds the inner $[Pt_{13}(CO)_{12}]^{2-}$ cluster as a pseudo π-allyl ligand, contributing three electrons (one per each Cd bonded to dmf). The overall electron count is still 162 CVE [13(Pt) × 10 + 12(CO) × 2 + 2(negative charge) + 2(Cd rings) × 3]. Based on the cluster-borane analogy, an icosahedral transition metal cluster should display 170 CVE rather than 162 CVE.[108] Nonetheless, most gold icosahedral clusters display 162 CVE, as in the case of $[Au_{13}Cl_2(PMe_2Ph)_{10}]^{3+}$ and $[Au_9M_4Cl_4(PMe_2Ph)_{10}]^{+}$ (M = Cu, Ag, Au).[109] Mingos rational-

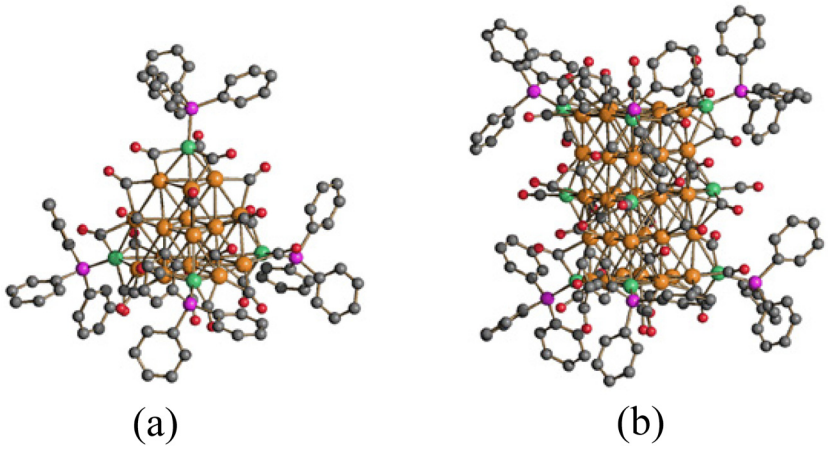

Fig. 10 MCCs decorated by Ni(PR$_3$) fragments: (a) $[Pd_{16}Ni_4(CO)_{22}(PPh_3)_4]^{2-}$ and (b) $[Pd_{33}Ni_9(CO)_{41}(PPh_3)_6]^{4-}$ (orange, Pd; green, Ni; purple, P; grey, C; red, O). H-atoms have been omitted for clarity.

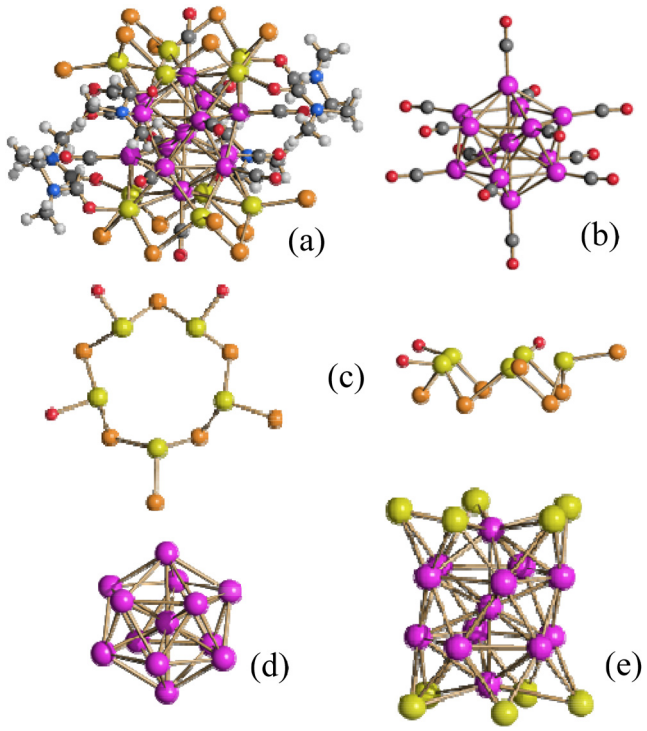

Fig. 11 $[Pt_{13}(CO)_{12}\{Cd_5(\mu\text{-}Br)_5Br_2(dmf)_3\}_2]^{2-}$ (a) may be described as composed of a $[Pt_{13}(CO)_{12}]^{8-}$ anionic core (b) decorated by two cationic $[\{Cd_5(\mu\text{-}Br)_5Br_2(dmf)_3\}]^{3+}$ rings (c, tow views). The resulting Pt_{13} and $Pt_{13}Cd_{10}$ cores are represented in (d) and (e), respectively (purple, Pt; yellow, Cd; orange, Br; blue, N; red, O; grey, C; white, H). Adapted with permission from ref. 106 Copyright 2011 American Chemical Society.

ized the low electron count of such clusters based on the predominance of radial over tangential bonding.[110] Pyykko further supported the explanation of Mingos, by performing DFT calculations of the hypothetical 162 CVE $[WAu_{12}(CO)_{12}]$ cluster.[111] The same electron count has been found also in $[Pt_{13}\{Au_2(PPh_3)_2\}_2(CO)_{10}(PPh_3)_4]$ (Fig. 12), composed of a $[Pt_{13}(CO)_{10}(PPh_3)_4]^{4-}$ core [13(Pt) × 10 + 10(CO) × 2 + 4(PPh_3) × 2 + 4(negative charge) = 162 CVE] decorated by two $[Au_2(PPh_3)_2]^{2+}$, acting as Lewis acids.[112] Using a similar approach based on Lewis Dot Formulas, staple motives such as $[Au(SR)_2]^-$ and $[Au_2(SR)_3]^-$, found in thiolated gold clusters, may be viewed essentially as four-electron donors. Within this framework, the $[Au_{25}(SCH_2CH_2Ph)_{18}]^-$ nanocluster may be viewed as composed of a $[Au_{13}]^{5+}$ core [13(Au) × 11 − 5(positive charge) = 138 CVE] and six $[Au_2(SR)_3]^-$ staple motives [contributing 6 × 4 = 24 CVE], with an overall electron count of 162 CVE, as in the above mentioned organometallic carbonyl and phosphine clusters.

Saillard *et al.* have analyzed the same clusters within the framework of the superatom model.[51] $[Au_{13}Cl_2(PMe_2Ph)_{10}]^{3+}$ is a superatom with 8 free electrons (fe = free electrons; nfe = number of free electrons) [nfe = 13(Au_{13}) − 2 (Cl_2) − 3(positive charge) = 8] and $1S^2\ 1P^6$ closed-shell configuration. In the case of $[Pt_{13}(CO)_{12}\{Cd_5(\mu\text{-}Br)_5Br_2(dmf)_3\}_2]^{2-}$, the 8− charge of the $[Pt_{13}(CO)_{12}]^{8-}$ core provides the 8 free electrons for the same superatomic $1S^2\ 1P^6$ configuration. This point has been further corroborated by the Kohn–Sham orbital diagram of $[Pt_{13}(CO)_{12}]^{8-}$, where the 1S and 1P orbitals lie at the bottom of the fully occupied 5d block, whereas the empty 1D level is located above the π*(CO) orbitals (Fig. 13). Similar conclusions apply to $[Pt_{13}\{Au_2(PPh_3)_2\}_2(CO)_{10}(PPh_3)_4]$, which is again a superatom with nfe = 8. These bonding analyses may be extended to other Pt–Cd carbonyl clusters, and the reader may find details in the cited literature.[51]

Surface decoration of MCCs with Lewis acids may be extended also to main group metal-based fragments. For instance, reactions of $[Ni_6(CO)_{12}]^{2-}$ with $InBr_3$ under different experimental conditions lead to the selective formation of $[Ni_6(\mu_3\text{-}InBr_3)(\eta^2\text{-}\mu_6\text{-}In_2Br_5)(CO)_{11}]^{3-}$, $[Ni_6(\eta^2\text{-}\mu_6\text{-}In_2Br_5)_2(CO)_{10}]^{4-}$, and $[Ni_{12}(\mu_6\text{-}In)(\eta^2\text{-}\mu_6\text{-}In_2Br_4OH)(CO)_{22}]^{4-}$ (Fig. 14).[113] These clusters are composed of $[Ni_6(CO)_{11}]^{4-}$ or $[Ni_6(CO)_{10}]^{6-}$ carbonyl cores decorated by Lewis-acid fragments such as $InBr_3$, $[In_2Br_5]^+$, $[In_2Br_4OH]^+$ and $[In]^{3+}$.

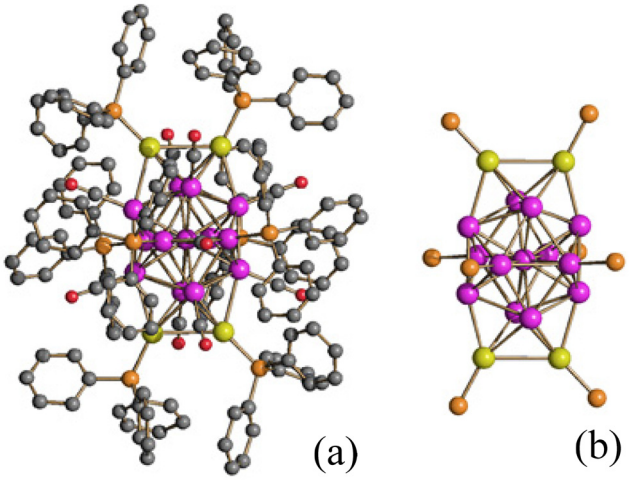

Fig. 12 $[Pt_{13}\{Au_2(PPh_3)_2\}_2(CO)_{10}(PPh_3)_4]$ (a) is composed of a $[Pt_{13}(CO)_{10}(PPh_3)_4]^{4-}$ core decorated by two $[Au_2(PPh_3)_2]^{2+}$ fragments (b) (purple, Pt; yellow, Au; orange, P; red, O; grey, C). H-atoms have been omitted for clarity in (a). CO ligands and Ph rings have been omitted in (b).

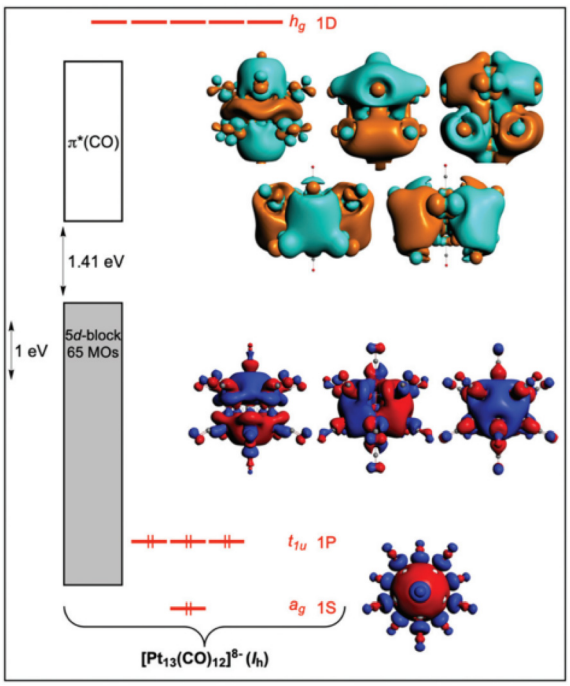

Fig. 13 Kohn–Sham MO diagram of $[Pt_{13}(CO)_{12}]^{8-}$, as found in the structure of $[Pt_{13}(CO)_{12}\{Cd_5(\mu\text{-}Br)_5Br_2(dmf)_3\}_2]^{2-}$. Adapted from ref. 51 with permission from The Royal Society of Chemistry.

2.2. Metal–ligand fragments as Lewis bases

Metal–ligand fragments with a Lewis base character may coordinate to the surface of a MCC as monodentate or polydentate ligands. Such fragments may replace one or more CO ligands in existing MCCs, or stabilize non-existing MCC cores. Therefore, these metal–ligand Lewis base fragments may be viewed as organometallic analogues of organic ligands, such as monodentate or polydentate phosphines.

Among these, Sn(II) based fragments are very effective and versatile. Simple fragments such as $[SnCl_3]^-$, $SnCl_2$ and $[SnCl]^+$ may be viewed as two-electron donor ligands, related to alkyl, carbene and carbyne ligands, respectively (Scheme 1). The $[Cl_2Sn(\mu\text{-}OR)SnCl_2]^-$ and $[Br_2Sn(\mu\text{-}Br)SnBr_2]^-$ fragments may be described as bidentate (four electron) ligands, whereas $[Cl_2SnOCOSnCl_2]^{2-}$ is a tridentate ligand, donating four electrons *via* the two Sn(II)-centers and two electrons *via* the C-atom. The species $[Pt_8(CO)_{10}(SnCl_2)_4]^{2-}$, $[Pt_5(CO)_5\{Cl_2Sn(OR)SnCl_2\}_3]^{3-}$ (R = H, Me, Et, ^{i}Pr), $[Pt_6(CO)_6(SnCl_2)_2(SnCl_3)_4]^{4-}$, $[Pt_9(CO)_8(SnCl_2)_3(SnCl_3)_2(Cl_2SnOCOSnCl_2)]^{4-}$ and $[Pt_{10}(CO)_{14}\{Cl_2Sn(OH)SnCl_2\}_2]^{2-}$ can be obtained from the reactions of $[Pt_{3n}(CO)_{6n}]^{2-}$ (n = 2–5) Chini clusters with $SnCl_2$ under different experimental conditions (Fig. 15).[114–116] These may be further transformed into $[Pt_6(CO)_8(SnCl_2)(SnCl_3)_4]^{4-}$ and $[Pt_6(CO)_8(SnCl_2)(SnCl_3)_2(PPh_3)_2]^{2-}$ upon reactions with CO and PPh_3. All these species may be viewed as Pt–CO clusters decorated by the above mentioned Sn-based fragments.

Reaction of $[Pt_{15}(CO)_{30}]^{2-}$ with $GeCl_4$ affords $[Pt_8(CO)_{10}(GeCl_2)_4]^{2-}$, isostructural to $[Pt_8(CO)_{10}(SnCl_2)_4]^{2-}$, that contains four carbene-like $GeCl_2$ ligands.[117] Several examples of Ru, Os and Ir carbonyl clusters decorated by $[GeR]^+$ and GeR_2 (R = H, alkyl, aryl) have been reported by Adams and Captain.[118–120] For instance, thermal reaction of $Ru_3(CO)_{12}$ and ^{t}BuGeH$_3$ in heptane affords a mixture of six clusters, that is, $Ru_3(CO)_9(\mu_3\text{-}Ge^tBu)_2$, $Ru_2(CO)_6(\mu\text{-}Ge^tBuH)_3$, $Ru_4(CO)_{10}(\mu_4\text{-}Ge_2{}^tBu_2)(\mu\text{-}Ge^tBuH)_2$, $Ru_4(CO)_8(\mu_4\text{-}Ge_2{}^tBu_2)(\mu\text{-}Ge^tBuH)_2(\mu_3\text{-}Ge^tBu)(H)$, $Ru_5(CO)_{12}(\mu_3\text{-}Ge^tBu)_2(\mu_4\text{-}Ge^tBu)(H)$, and $Ru_6(CO)_{12}(\mu_3\text{-}Ge^tBu)_4(H)_2$, which can be separated by TLC (Scheme 2). All these Ru–Ge carbonyl clusters are composed of Ru_2, Ru_3, Ru_4, Ru_5 and Ru_6 carbonyl cores decorated by $[Ge^tBu]^+$ and Ge^tBuH ligands.

The clusters $[Rh_6(CO)_{15}(GaCp^*)]$, $[Rh_6(CO)_{14}(GaCp^*)_2]$, $[Rh_6(CO)_{13}(GaCp^*)_3]$, and $[Rh_6(CO)_{12}(GaCp^*)_4]$ may be viewed as octahedral Rh_6 clusters decorated by GaCp* fragments (Fig. 16).[121,122] This is a two-electron donor fragment and, thus, these species are formally obtained upon replacement of 1–4 CO ligands in $[Rh_6(CO)_{16}]$ by 1–4 GaCp*. A related InCp* species has been also reported, that is, $[Rh_6(CO)_{15}(InCp^*)]$. The cluster $[Ni_4(CO)_6(GaCp^*)_4]$ is a tetrahedral 60 CVE species, analogue to the homoleptic $[Ni_4(CO)_{10}]$ cluster, which has never been observed (Fig. 17).[123]

3. Metal core decorated on the surface by metal-carbonyl fragments

Metal-carbonyl fragments may behave as ligands and coordinate to single metal ions, dimers or metal clusters. This applies to monometallic M–CO fragments, that is, $[M(CO)_n]^{z-}$, or polynuclear MCC fragments, that is, $[M_m(CO)_n]^{z-}$. Such M–CO fragments may exist or not exist as free species.

There are several complexes where a single d^{10} metal ion (Cu^+, Ag^+, Au^+, Zn^{2+}, Cd^{2+}, Hg^{2+}) is linearly bonded to two

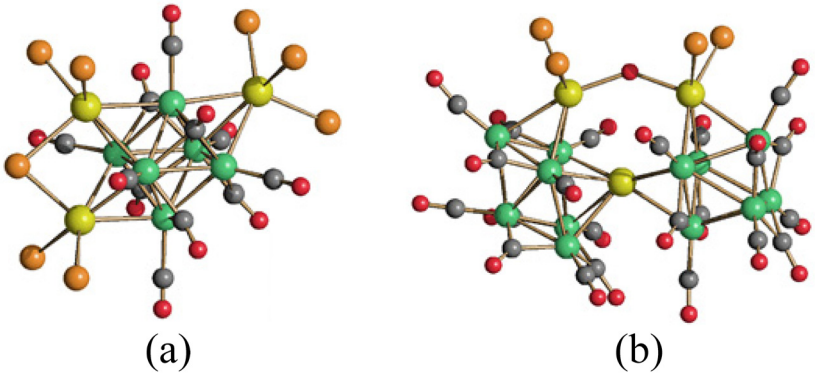

Fig. 14 MCCs decorated by main group metal-based fragments acting as Lewis acids. Molecular structures of (a) $[Ni_6(\mu_3\text{-}InBr_3)(\eta^2\text{-}\mu_6\text{-}In_2Br_5)(CO)_{11}]^{3-}$, and (b) $[Ni_{12}(\mu_6\text{-}In)(\eta^2\text{-}\mu_6\text{-}In_2Br_4OH)(CO)_{22}]^{4-}$ (green, Ni; yellow, In; orange, Br; red, O; grey, C). The H-atom of the OH group has not been located.

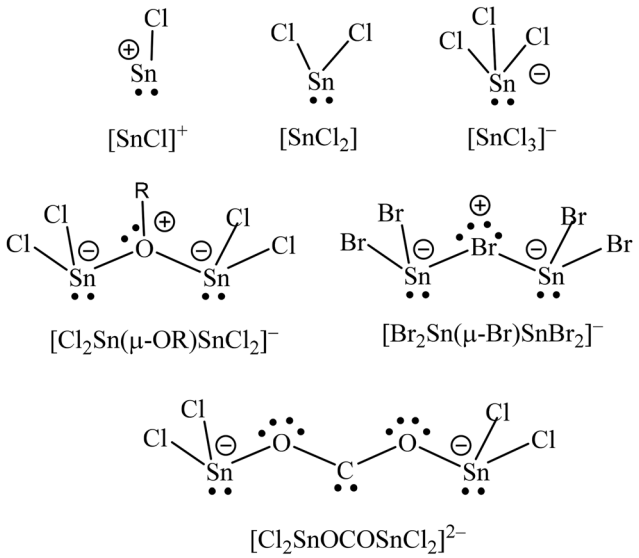

Scheme 1 Lewis dot formulas of the $[SnCl]^+$, $SnCl_2$, $[SnCl_3]^-$, $[Cl_2Sn(\mu\text{-}OR)SnCl_2]^-$, $[Br_2Sn(\mu\text{-}Br)SnBr_2]^-$ and $[Cl_2SnOCOSnCl_2]^{2-}$ ligands found in Pt carbonyl clusters decorated by Sn-fragments acting as Lewis bases.

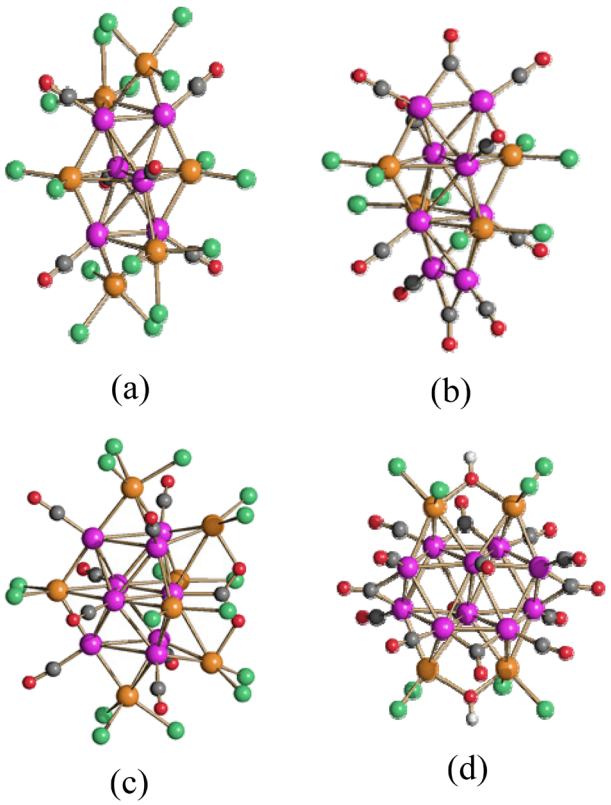

Fig. 15 Pt carbonyl clusters decorated by Sn-fragments acting as Lewis bases. Molecular structures of (a) $[Pt_6(CO)_6(SnCl_2)_2(SnCl_3)_4]^{4-}$, (b) $[Pt_8(CO)_{10}(SnCl_2)_4]^{2-}$, (c) $[Pt_9(CO)_8(SnCl_2)_3(SnCl_3)_2(Cl_2SnOCOSnCl_2)]^{4-}$ and (d) $[Pt_{10}(CO)_{14}\{Cl_2Sn(OH)SnCl_2\}_2]^{2-}$ (purple, Pt; orange, Sn; green, Cl; red, O; grey, C; white, H). Adapted from ref. 115 with permission from The Royal Society of Chemistry.

MCC fragments. Some noticeable examples are represented in Fig. 18.[124–126] Such complexes are closely related to MCCs decorated on the surface by ML fragments. In the case of compounds described in section 2.1, the central ion is bonded to one MCC fragment and one L (or X^-) ligand, whereas in the cases reported in Fig. 18, M is bonded to two MCC fragments.

In most of the cases so far reported, the single metal ion is coordinated to anionic MCC fragments. An interesting exception is represented by $[MFe_2(CO)_{10}]^+$ (M = Cu, Ag, Au), where the M^+ ions are linearly bonded to two neutral $Fe(CO)_5$ molecules.[127] There are also a few examples where a d^{10} ion is coordinated to extended cyclic or acyclic MCC fragments, such as $[MRu_6(CO)_{22}]^-$ (M = Cu, Ag), $[AuRu_5(CO)_{19}]^-$,[128] and $[HgOs_6(\mu\text{-}PPh_2)_2(CO)_{20}]$.[129]

In all cases, the MCC fragments act as Lewis bases, and they can also bind to larger M_n fragments. This point is well exemplified by the Hg–Ru clusters $[HgRu_6(CO)_{22}]^{2-}$, $[Hg_2Ru_7(CO)_{26}]^{2-}$, $[Hg_3Ru_8(CO)_{30}]^{2-}$, and $[Hg_4Ru_{10}(CO)_{32}]^{4-}$ (Fig. 19).[130] These contain $[Hg]^{2+}$, $[Hg_2]^{4+}$, linear $[Hg_3]^{6+}$, and rectangular $[Hg_4]^{8+}$ cores, respectively, stabilized by $[Ru(CO)_4]^{2-}$, $[Ru_3(CO)_{11}]^{2-}$, and $[Ru_4(CO)_{12}]^{2-}$ MCC anions. Triangular $[Hg_3]^{6+}$ cores have been found in $[Hg_3Os_9(CO)_{33}]$ and $[Hg_3Os_{18}(C)_2(CO)_{42}]^{2-}$ (Fig. 20).[131,132] The former cluster

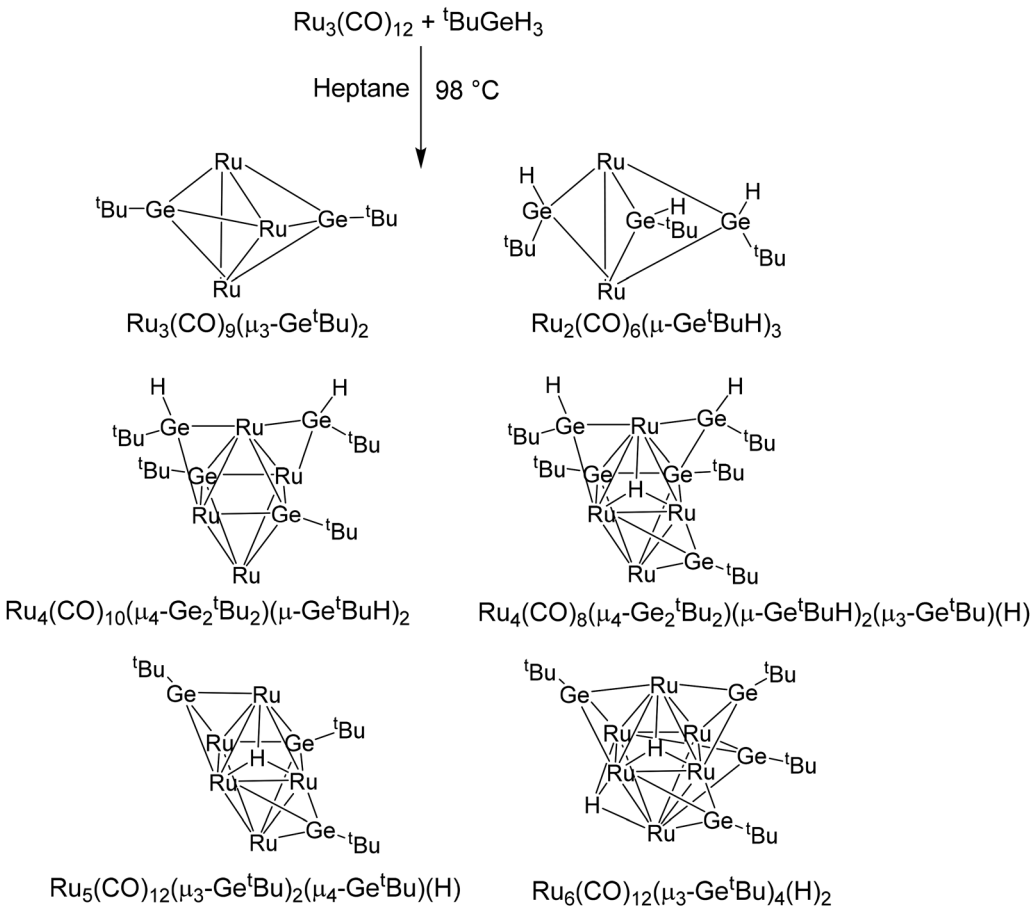

Scheme 2 The products of the thermal reaction of $Ru_3(CO)_{12}$ and $^tBuGeH_3$. The products have been separated by thin layer chromatography (TLC). CO ligands have been omitted for clarity. Adapted from ref. 9 with permission from The Royal Society of Chemistry.

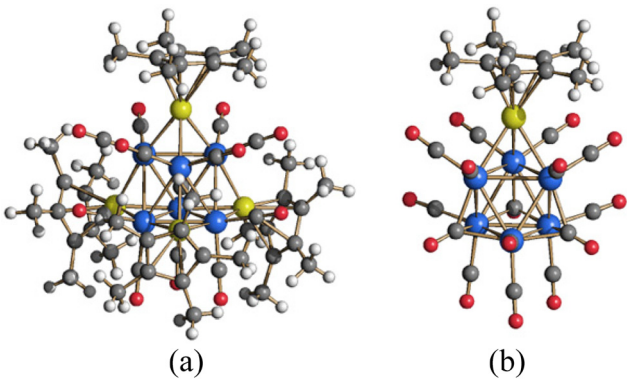

Fig. 16 Octahedral Rh carbonyl clusters decorated by GaCp* and InCp* fragments. Molecular structures of (a) $[Rh_6(CO)_{12}(\mu_3\text{-GaCp*})_4]$ and (b) $[Rh_6(CO)_{15}(\mu_3\text{-InCp*})]$ (blue, Rh; yellow, Ga (a) or In (b); red, O; grey, C; white, H). These compounds have been obtained upon reactions of $[Rh_6(CO)_{16}]$ with GaCp* and $[Rh_6(CO)_{15}(MeCN)]$ with InCp*, respectively (Cp* = pentamethylcyclopentadienyl). Adapted from ref. 9 with permission from The Royal Society of Chemistry.

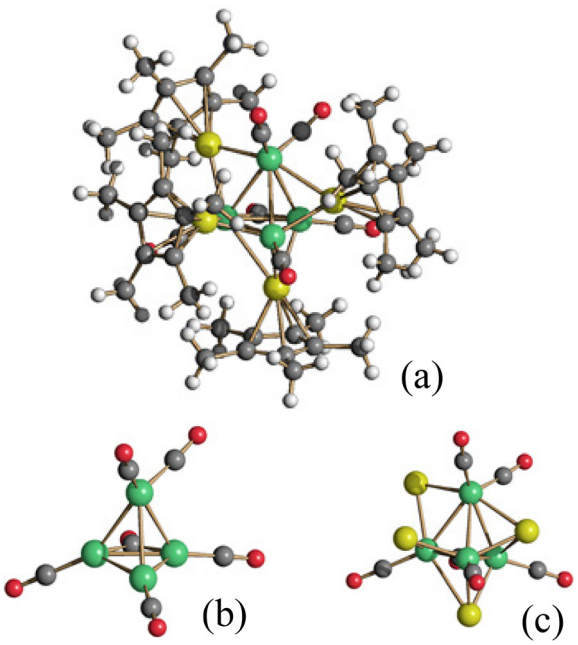

Fig. 17 The tetrahedral 60 CVE $[Ni_4(CO)_6(GaCp*)_4]$ cluster (a), composed of a $[Ni_4(CO)_6]$ core (b) decorated by four GaCp* fragments. The resulting $[Ni_4(CO)_6Ga_4]$ framework is represented in (c) (green, Ni; yellow, Ga; red, O; grey, C; white, H).

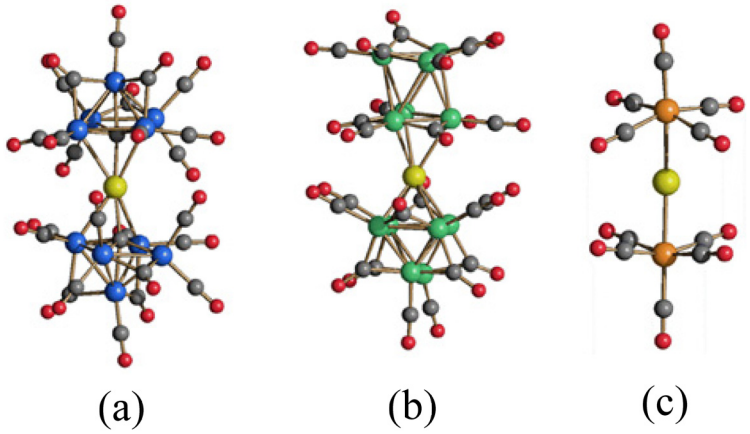

Fig. 18 Single metal ions stabilised upon coordination to metal carbonyl fragments. Molecular structures of (a) $[\{Co_5C(CO)_{12}\}_2Au]^-$, (b) $[\{Ni_6(CO)_{12}\}_2Au]^{3-}$, and (c) $[\{Fe(CO)_5\}_2Au]^+$ (blue, Co; green, Ni; orange, Fe; yellow, Au; red, O; grey, C).

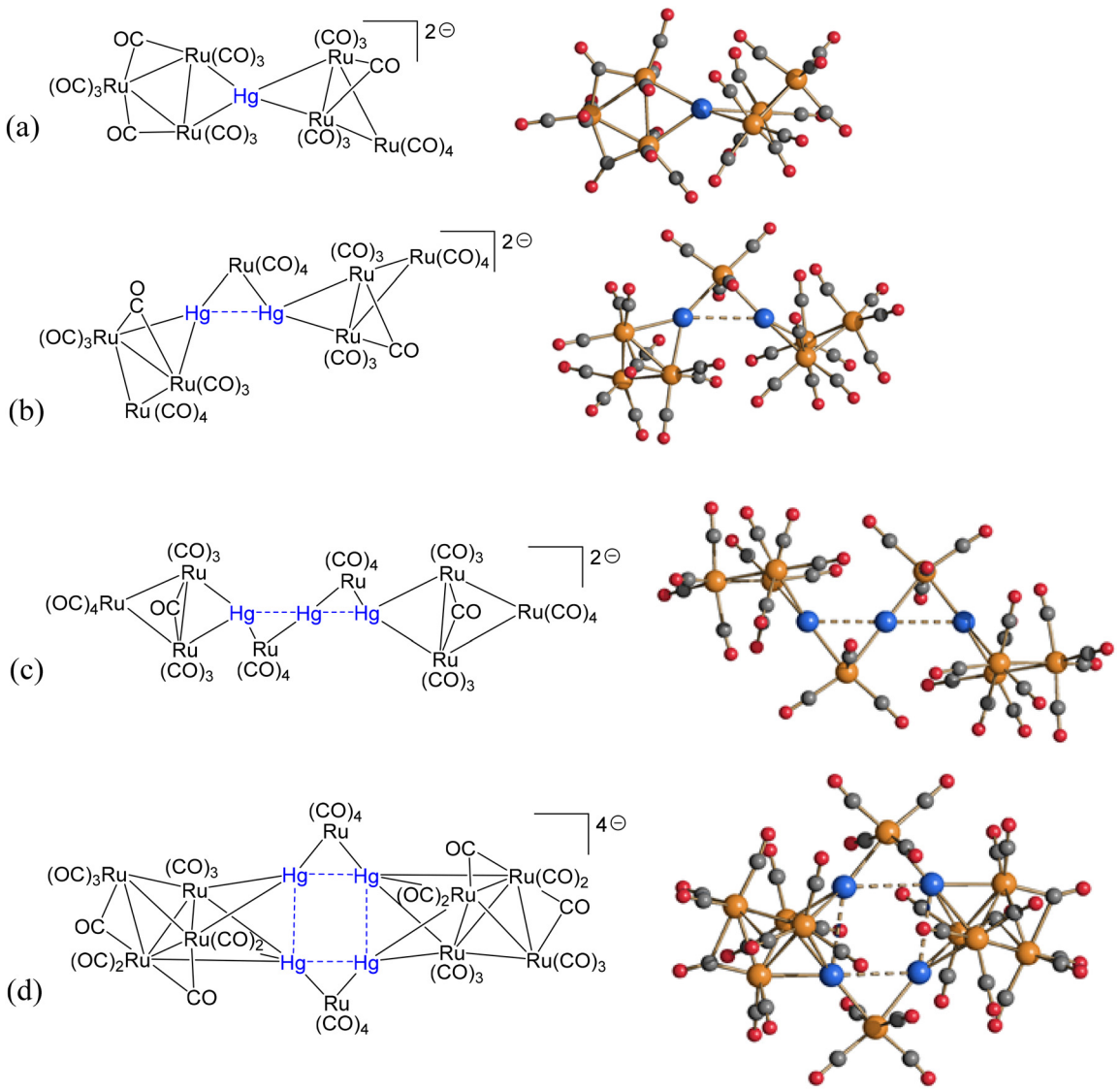

Fig. 19 $[Hg_n]^{2n+}$ (n = 1–4) cores stabilised upon coordination to metal carbonyl fragments. Molecular structures of (a) $[HgRu_6(CO)_{22}]^{2-}$, (b) $[Hg_2Ru_7(CO)_{26}]^{2-}$, (c) $[Hg_3Ru_8(CO)_{30}]^{2-}$, and (d) $[Hg_4Ru_{10}(CO)_{32}]^{4-}$ (blue, Hg; orange, Ru; red, O; grey, C). Adapted from ref. 130 with permission from Elsevier.

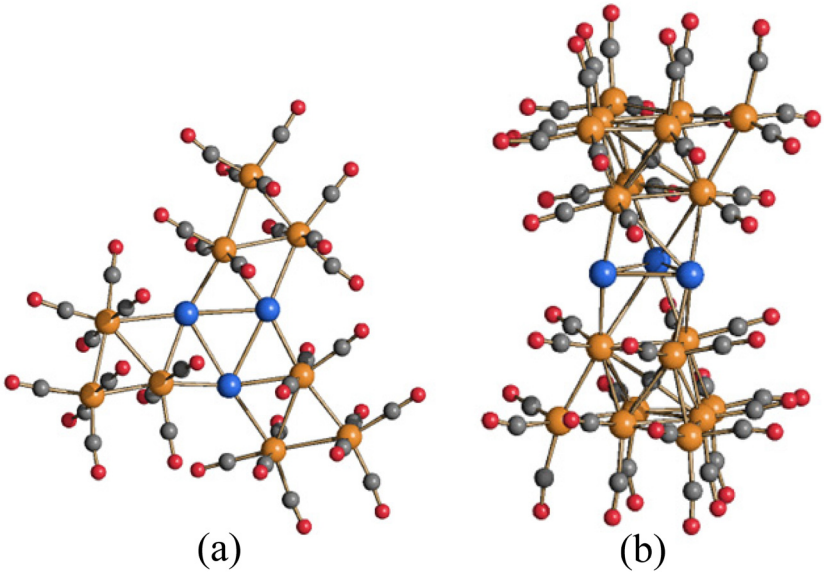

Fig. 20 (a) The triangular $[Hg_3]^{6+}$ unit can be stabilised upon coordination of three $[Os_3(CO)_{11}]^{2-}$ MCCs on its three edges resulting in the 2-D surface decorated MCC $[Hg_3Os_9(CO)_{33}]$. (b) Alternatively, it can be sandwiched between two $[Os_9C(CO)_{21}]^{4-}$ MCCs, resulting in $[Hg_3Os_{18}(C)_2(CO)_{42}]^{2-}$ (blue, Hg; orange, Os; red, O; grey, C).

possesses a slightly twisted 2-D structure, since the three $[Os_3(CO)_{11}]^{2-}$ units are side-by-side bonded to the three edges of the $[Hg_3]^{6+}$ triangle. Conversely, in the case of $[Hg_3Os_{18}(C)_2(CO)_{42}]^{2-}$, the two $[Os_9C(CO)_{21}]^{4-}$ fragments are bonded to the two triangular faces of $[Hg_3]^{6+}$, resulting in a sandwich compound. Mercurophilic interactions are present in all these compounds.

Square or rectangular $[M_4]^{n+}$ cores (n = 4, M = Cu, Ag, Au; n = 8, M = Cd, Hg) stabilized by MCC fragments are rather common. Representative examples are $[M_4Fe_4(CO)_{16}]^{4-}$ (M = Ag, Au),[133] $[M_4Co_4(CO)_{16}]$,[63] (M = Cu, Ag), $[M_4Mo_4(Cp)_4(CO)_{12}]$ (M = Ag, Au), $[M_4Mo_4(C_5H_4NMe_2)_4(CO)_{12}]$ (M = Ag, Au),[134] $[Cd_4Fe_4(CO)_{16}]$, $[Hg_4Ru_4(CO)_{16}]$,[135] and $[Hg_4Mn_4(MeCp)_4(CO)_8]$ (Fig. 21).[136] These 2-D clusters contain $[M_4]^{4+}$ (M = Cu, Ag, Au) or $[M_4]^{8+}$ (M = Cd, Hg) cores stabilized by $[Fe(CO)_4]^{2-}$, $[Ru(CO)_4]^{2-}$, $[Co(CO)_4]^{-}$, $[CpMo(CO)_3]^{-}$, and $[(MeCp)Mn(CO)_2]^{2-}$ fragments. Anionic $[M_4Fe_4(CO)_{16}]^{4-}$ (M = Ag, Au) may be further decorated by $[Au_2(dppm)]^{2+}$ and $[Au_2(dppe)]^{2+}$ fragments affording the larger 2-D clusters $[Ag_8Fe_4(CO)_{16}(dppm)_2]$, $[Ag_4Au_4Fe_4(CO)_{16}(dppe)_2]$, $[Au_8Fe_4(CO)_{16}(dppe)_2]$, and, $[Au_6Cu_2Fe_4(CO)_{16}(dppe)_2]$.[137,138] The species $[Au_8Mo_4(CO)_{20}(PPh_3)_4]$ is closely related.[139]

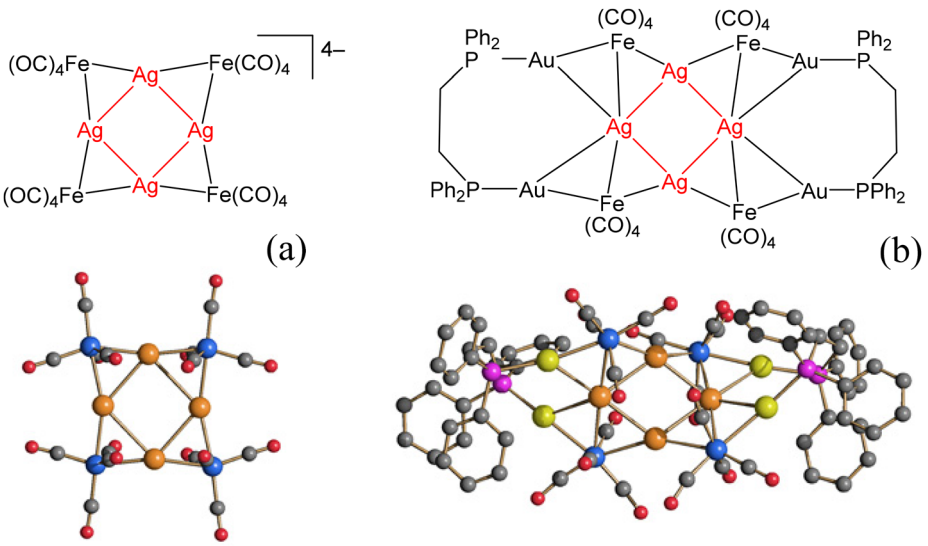

Fig. 21 MCCs based on square $[Ag_4]^{4+}$ cores stabilised upon coordination of four $[Fe(CO)_4]^{2-}$ units, which can be further decorated by two $[Au_2(dppe)]^{2+}$ fragments. Molecular structures of (a) $[Ag_4Fe_4(CO)_{16}]^{4-}$ and (b) $[Ag_4Au_4Fe_4(CO)_{16}(dppe)_2]$ (blue, Fe; orange, Ag; yellow, Au, purple, P; red, O; grey, C). Hydrogen atoms have been omitted.

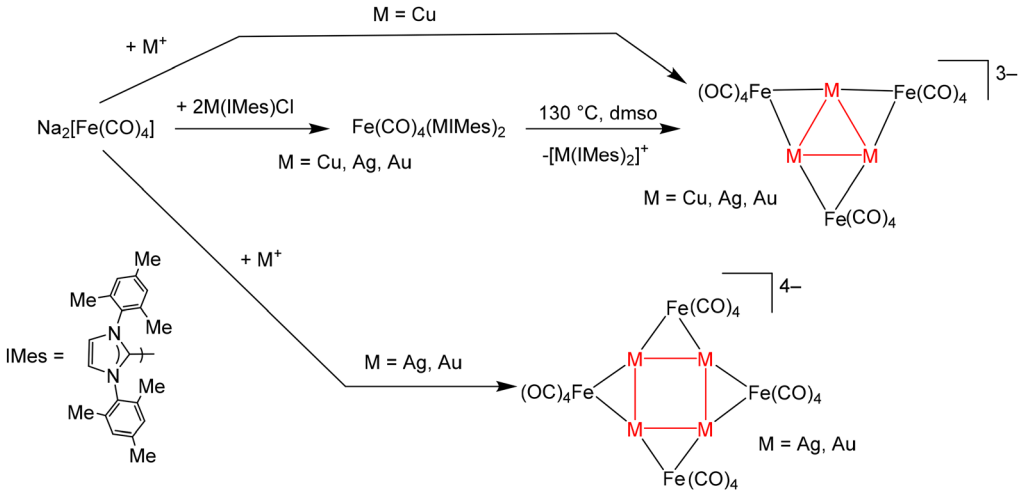

Scheme 3 Syntheses of the clusters $[M_3Fe_3(CO)_{12}]^{3-}$ (M = Cu, Ag, Au) and $[M_4Fe_4(CO)_{16}]^{4-}$ (M = Ag, Au). In the case of Ag and Au, the trimeric and tetrameric clusters may be viewed as polymerization isomers. Adapted with permission from ref. 133 Copyright 2019 American Chemical Society.

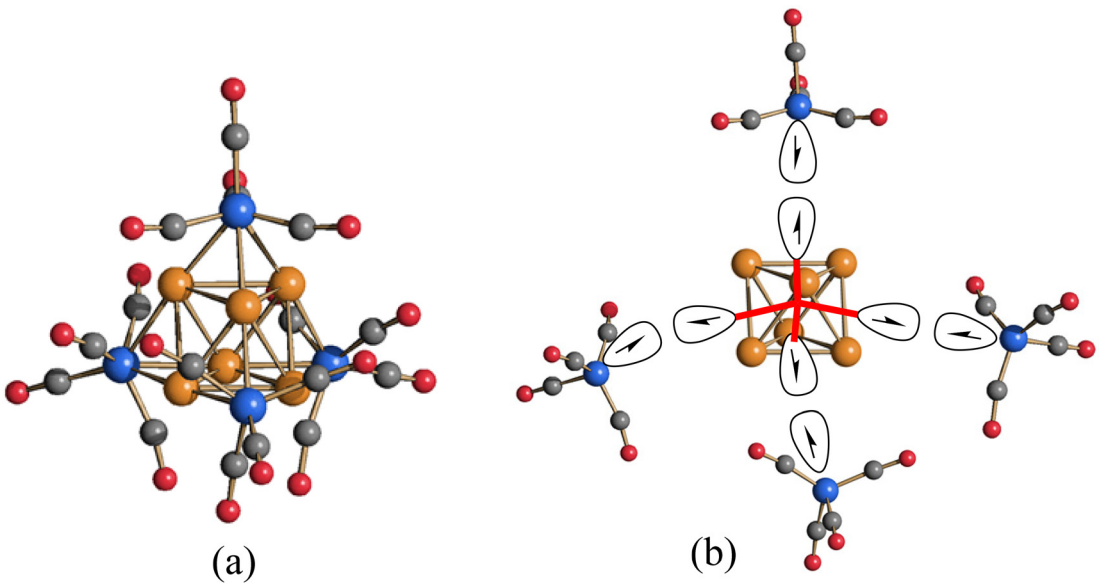

Fig. 22 (a) The molecular cluster $[Cu_6Fe_4(CO)_{16}]^{2-}$ may be viewed as (b) a sp^3 four-electron $[Cu_6]^{2+}$ superatom bonded to four $[Fe(CO)_4]^{\bullet-}$ MCC radical fragments (blue, Fe; orange, Cu; red, O; grey, C).

Polymerization isomerism has been observed in the case of $[M_4Fe_4(CO)_{16}]^{4-}$ (M = Ag, Au). Indeed, it has been possible to synthesize and structurally characterize their triangular isomers $[M_3Fe_3(CO)_{12}]^{3-}$ (M = Ag, Au) (Scheme 3).[133] Conversely, only $[Cu_3Fe_3(CO)_{12}]^{3-}$ is known in the case of copper.

The species $[M_5Fe_4(CO)_{16}]^{3-}$ (M = Cu, Ag, Au) contain a centered rectangular $[M_5]^{5+}$ core decorated on the surface by four $[Fe(CO)_4]^{2-}$ fragments, and formally originate upon addition of a M^+ ion at the center of $[M_4Fe_4(CO)_{16}]^{4-}$. Interestingly, complex mixtures of 2-D molecular alloy clusters of the type $[M_xM'_{5-x}Fe_4(CO)_{16}]^{3-}$ (M, M′ = Cu, Ag, Au; M ≠ M′) can be prepared in an almost continuum of compositions.[140]

In the case of copper, further addition of a Cu^+ ion affords the 3-D cluster $[Cu_6Fe_4(CO)_{16}]^{2-}$, composed of an octahedral $[Cu_6]^{6+}$ core and four $[Fe(CO)_4]^{2-}$ fragments. Alternatively, this cluster may be viewed as a sp^3 four-electron $[Cu_6]^{2+}$ superatom bonded to four $[Fe(CO)_4]^{\bullet-}$ MCC radical fragments (Fig. 22). The same model has been applied to anionic $[Au_6Ni_{12}(CO)_{24}]^{2-}$ and cationic $[Ag_6M_4(CO)_{24}]^{2+}$ (M = Nb, Ta), which contain a $[M_6]^{2+}$ (M = Ag, Au) superatom tetrahedrally bonded to four $[Ni_3(CO)_6]^{\bullet-}$ or four $[M(CO)_6]^{\bullet}$ (M = Nb, Ta) radical metal carbonyl fragments (Fig. 23 and 24).[52,53] The closely related $[Ag_6Nb_5(CO)_{30}]^+$ has been interpreted as composed of a trigonal prismatic $[Ag_6]^+$ five electrons core bonded to five [Nb

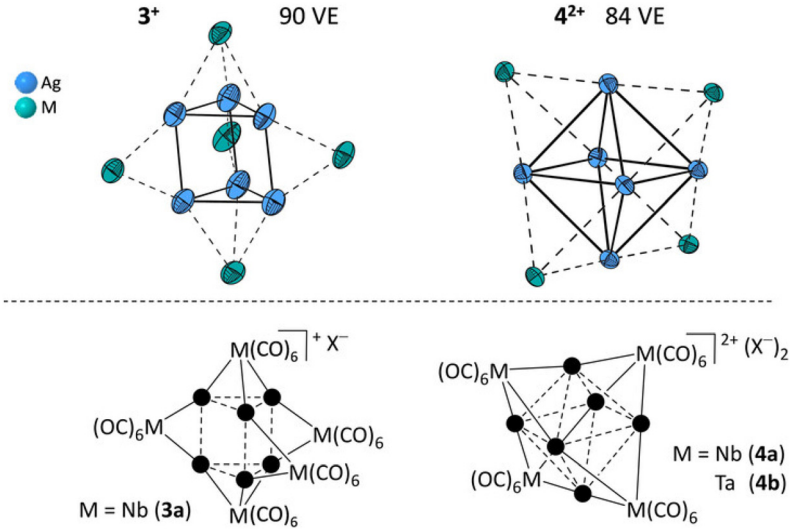

Fig. 23 Schematic structural formulae and structures of the metallic cores of the cationic cluster cores of $[Ag_6Nb_5(CO)_{30}]^+$ ($\mathbf{3}^+$) and $[Ag_6M_4(CO)_{24}]^{2+}$ (M = Nb, Ta) ($\mathbf{4}^{2+}$). The counterions $[Al(OR^F)_4]^-$ and the CO ligands are omitted for clarity in all structures. Ellipsoids were drawn at the 50 % probability level. Sum of the formally available valence electrons (VE) of the metal cores (Ag^+: 10 VE and M^-: 6 VE). Adapted from ref. 52 with permission from Wiley.

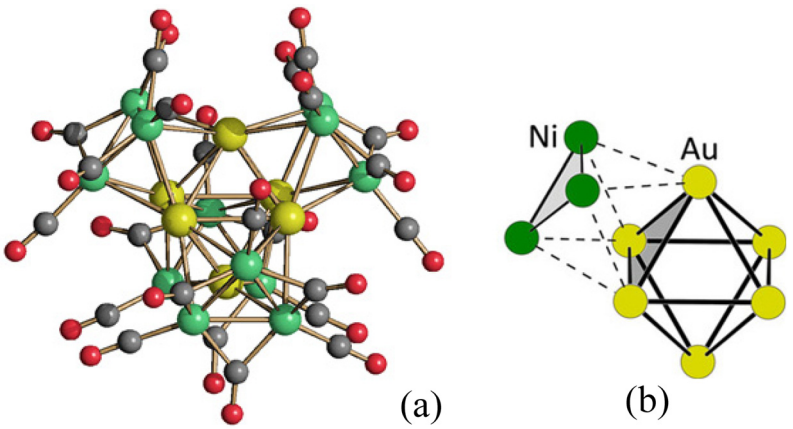

Fig. 24 The molecular cluster $[Au_6Ni_{12}(CO)_{24}]^{2-}$ (a) may be viewed as a sp^3 four-electron $[Au_6]^{2+}$ superatom bonded to four $[Ni_3(CO)_6]^{\bullet-}$ MCC radical fragments (green, Ni; yellow, Au; red, O; grey, C). The interaction of one of these radical fragments with the octahedral core is schematically represented (b). Adapted from ref. 52 with permission from Wiley.

$(CO)_6]^{\bullet}$ radicals, which adopt a trigonal bypiramidal arrangement. Octahedral cores have been found also in $[Au_6Rh_{16}(CO)_{36}]^{6-}$ and $[HPd_6Fe_6(CO)_{24}]^{3-}$,[141,142] but theoretical studies for their possible rationalization within the superatom model have not been yet carried out.

A further intriguing example where M–CO fragments act as ligands toward a gold cluster is $[Au_6Co_2(PPh_3)_4(CO)_8]$.[143] Its $[Au_6]^{2+}$ core consists of two tetrahedra with a common edge, bonded to four PPh_3 and two $[Co(CO)_4]^-$ units all acting as terminal ligands. Alternatively, it could be interpreted as composed of a neutral $[Au_6]$ core, four PPh_3 ligands and two $[Co(CO)_4]^{\bullet}$ radicals.

A few examples of larger nanoclusters containing metal cores decorated by MCC fragments have been reported, that is, $[Ag_9Os_{13}(CO)_{48}]^-$, $[Ag_9Os_9(\mu_3\text{-}O)_2(CO)_{30}]^-$,[144] $[Ag_{13}Fe_8(CO)_{32}]^{n-}$ (n = 3, 4, 5),[140] $[Ag_{16}Ni_{24}(CO)_{40}]^{4-}$,[145] $[H_{3-n}Pd_9Co_{15}C_3(CO)_{38}]^{n-}$ (n = 0–3), $[H_{6-n}Pd_{16}Co_{20}C_4(CO)_{48}]^{n-}$ (n = 3–6),[146–148] $[Au_{21}Fe_{10}(CO)_{40}]^{5-}$, $[Au_{22}Fe_{12}(CO)_{48}]^{6-}$, $[Au_{28}Fe_{14}(CO)_{52}]^{8-}$, and $[Au_{34}Fe_{14}(CO)_{50}]^{10-}$.[149]

The two Ag–Os clusters are actually composed of three $[Ag_3]^{3+}$ units stabilized upon coordination to four $[Os_3(CO)_{11}]^{2-}$ and one $[Os(CO)_4]^{2-}$ fragments in the case of $[Ag_9Os_{13}(CO)_{48}]^-$, and two $[Os_3O(CO)_9]^{2-}$ and three $[Os(CO)_4]^{2-}$ units in the case of $[Ag_9Os_9(\mu_3\text{-}O)_2(CO)_{30}]^-$.[144]

The very impressive $[Ag_{16}Ni_{24}(CO)_{40}]^{4-}$ cluster reported by Dahl *et al.*,[145] is composed of a *ccp* Ag_{16} kernel whose surface is connected to four tetrahedrally disposed triangular $Ni_6(CO)_{10}$ fragments. Taking into consideration the negative

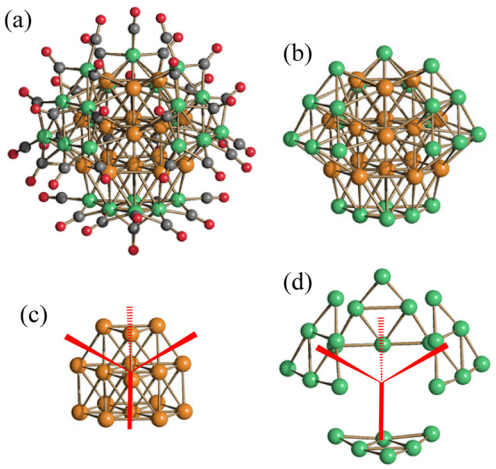

Fig. 25 The molecular structure of the cluster $[Ag_{16}Ni_{24}(CO)_{40}]^{4-}$ (a), whose $Ag_{16}Ni_{24}$ metal kernel (b) may be derived from the interaction of a *ccp* Ag_{16} core (c) with four $[Ni_6(CO)_{10}]^{\bullet-}$ radicals (d), adopting a tetrahedral arrangement (green, Ni; orange, Ag; red, O; grey, C).

charge, it may be viewed as a 16 electrons Ag_{16} core bonded to four $[Ni_6(CO)_{10}]^{\bullet-}$ radicals (Fig. 25).

$[H_{3-n}Pd_9Co_{15}C_3(CO)_{38}]^{n-}$ (n = 0–3) and $[H_{6-n}Pd_{16}Co_{20}C_4(CO)_{48}]^{n-}$ (n = 3–6) display some interesting features (Fig. 26).[146–148] First of all, they are composed of compact Pd_9 and Pd_{16} cores decorated by three or four $[Co_5C(CO)_{12}]$ MCC fragments arranged in a trigonal planar and tetrahedral geometry, respectively (Fig. 27). Moreover, they are poly-hydrides and each single hydride species display some reversible redox processes, as assessed by electrochemical studies. SQUID measurements indicate that $[HPd_9Co_{15}C_3(CO)_{38}]^{2-}$ is paramagnetic with two unpaired electrons. The structure of the Pd_9 core of $[H_{3-n}Pd_9Co_{15}C_3(CO)_{38}]^{n-}$ (n = 0–3) reversibly changes from trigonal prismatic to octahedral upon protonation/deprotonation reactions. Core isomerism has been observed in the case of $[HPd_9Co_{15}C_3(CO)_{38}]^{2-}$ that may adopt both trigonal prismatic and octahedral structures of the Pd_9 core, depending on packing forces.

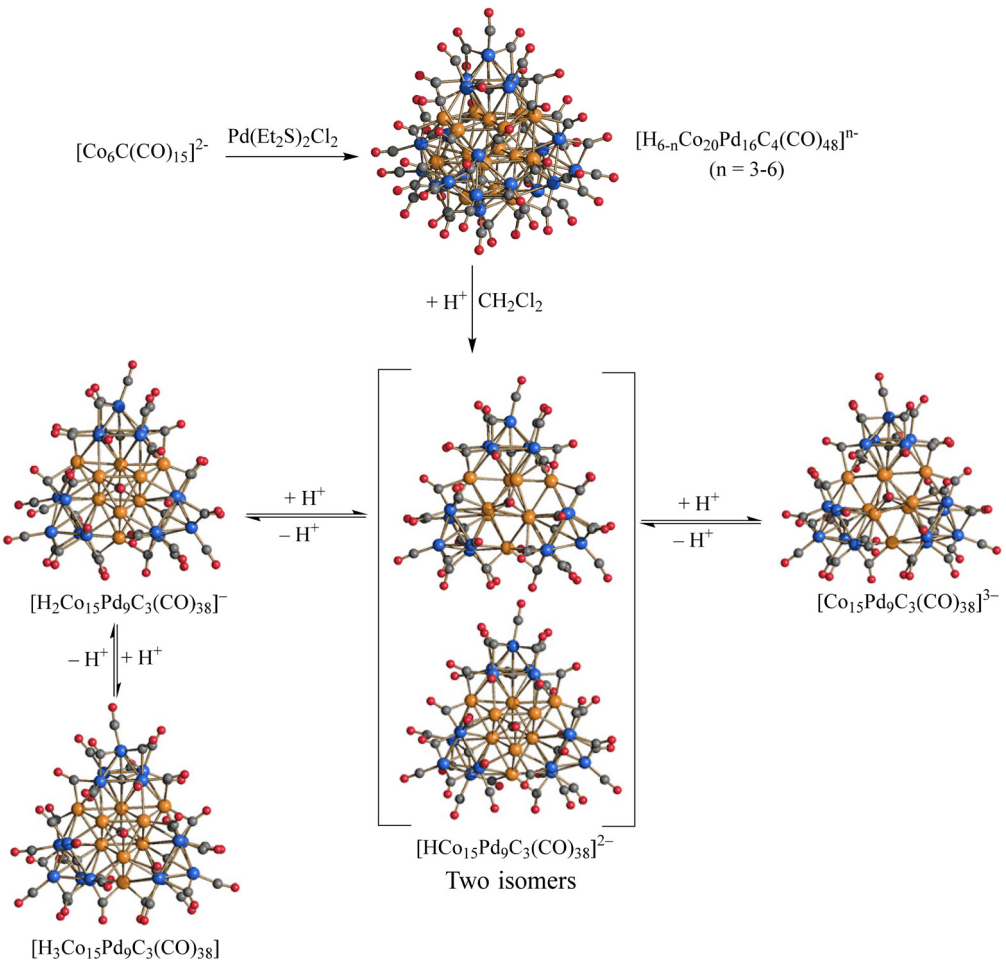

Fig. 26 Synthesis of $[H_{6-n}Co_{20}Pd_{16}C_4(CO)_{48}]^{n-}$ (n = 3–6) and its transformation into $[HPd_9Co_{15}C_3(CO)_{38}]^{2-}$ upon reaction with HBF_4 in CH_2Cl_2. Protonation/deprotonation reactions of $[H_{3-n}Co_{15}Pd_9C_3(CO)_{38}]^{n-}$ (n = 0–3) are reported. $[H_3Co_{15}Pd_9C_3(CO)_{38}]$ and $[H_2Co_{15}Pd_9C_3(CO)_{38}]^{-}$ display an Oh-Pd_9 core, whereas $[Co_{15}Pd_9C_3(CO)_{38}]^{3-}$ adopt a TP-Pd_9 structure (Oh = octahedron; TP = trigonal prism). Both isomers have been found in the case of $[HCo_{15}Pd_9C_3(CO)_{38}]^{2-}$ (orange, Pd; blue, Co; red, O; grey, C). Hydride ligands have not been located by SC-XRD. Adapted from ref. 147 with permission from The Royal Society of Chemistry.

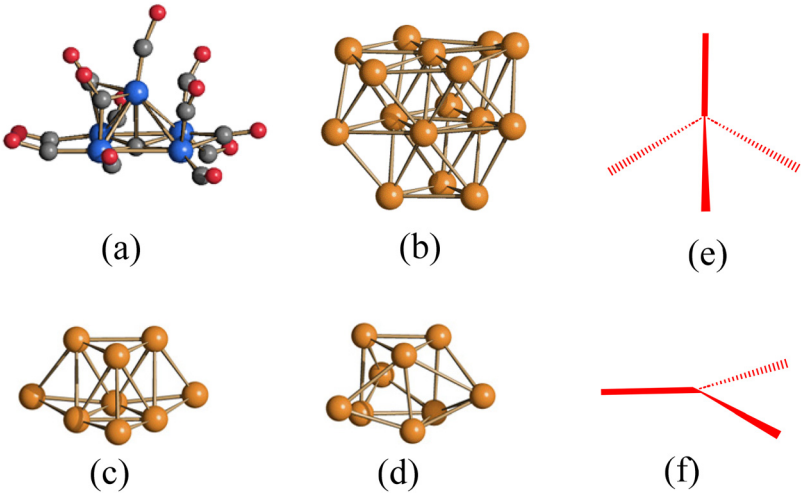

Fig. 27 Schematic representation of (a) one of the $[Co_5C(CO)_{12}]$ fragment decorating the $[H_{3-n}Pd_9Co_{15}C_3(CO)_{38}]^{n-}$ (n = 0–3) and $[H_{6-n}Pd_{16}Co_{20}C_4(CO)_{48}]^{n-}$ (n = 3–6) clusters, and their (b) Pd_{16}, (c) octahedral Pd_9 and (d) trigonal prismatic Pd_9 cores. The tetrahedral and trigonal planar arrangements of the $[Co_5C(CO)_{12}]$ fragments around these Pd_n cores is represented in (e) and (f).

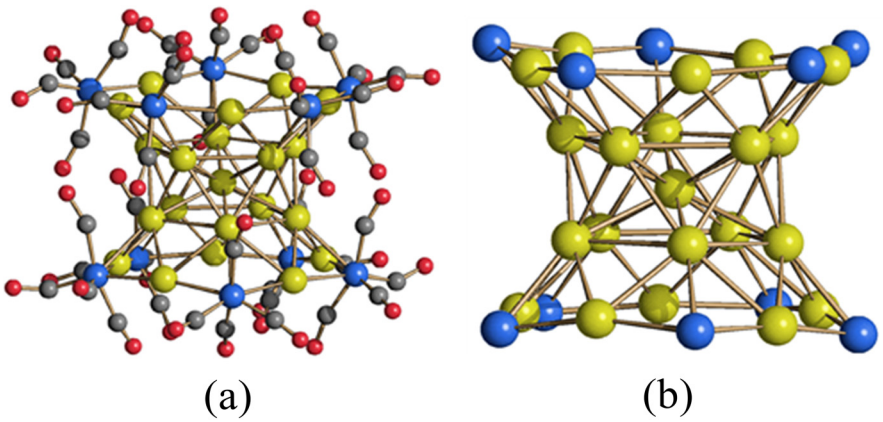

Fig. 28 Molecular structure (a) and metal core (b) of $[Au_{21}Fe_{10}(CO)_{40}]^{5-}$ (yellow, Au; blue, Fe; grey, C; red, O). The central $[Au_{11}]^{5+}$ unit is bonded to two $[Au_5\{\mu\text{-}Fe(CO)_4\}_5]^{5-}$ rings containing linear Fe–Au–Fe motives.

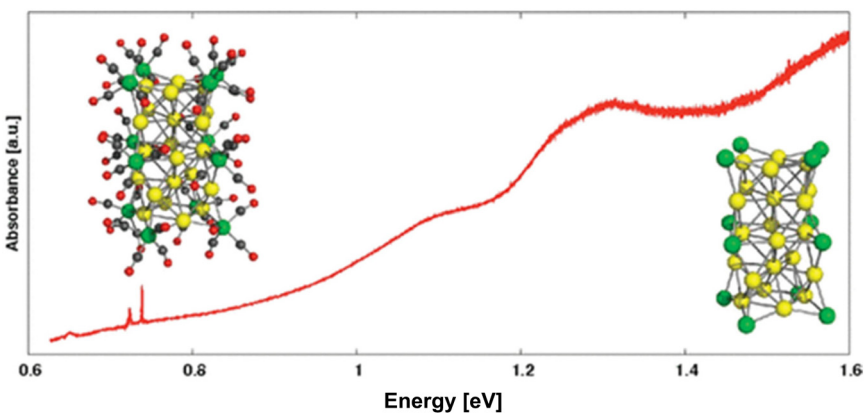

Fig. 29 NIR absorption spectrum recorded in CH_3CN, molecular structure and $Au_{22}Fe_{12}$ frame of $[Au_{22}Fe_{12}(CO)_{48}]^{6-}$ (yellow, Au; green, Fe; grey, C; red, O). Adapted with permission from ref. 50 Copyright 2009 American Chemical Society.

The $[Au_{21}Fe_{10}(CO)_{40}]^{5-}$, $[Au_{22}Fe_{12}(CO)_{48}]^{6-}$, $[Au_{28}Fe_{14}(CO)_{52}]^{8-}$, and $[Au_{34}Fe_{14}(CO)_{50}]^{10-}$ nanoclusters may be viewed as organometallic counterparts of thiolate-protected gold nanoclusters.[149] Indeed, these Au–Fe–CO molecular nanoclusters are stabilized on the surface by linear Fe–Au–Fe fragments, reminiscent of the S–Au–S staple motives present in ligand protected Au nanoclusters. Because of this, the real nuclearity of the metal cores of such Au–Fe–CO and Au–SR nanoclusters are reduced compared to the nominal ones. The linear fragments on the surface may generate larger motives, such as Au$(SR)_2$ and $Au_2(SR)_3$ in the case of Au–SR nanoclusters, and Au$\{Fe(CO)_4\}_2$ and $Au_2\{Fe(CO)_4\}_3$ for Au–Fe–CO MCCs. Both an ionic and neutral model may be used in order to interpret their bonding. Using the ionic model, $[Au_{21}Fe_{10}(CO)_{40}]^{5-}$ may be partitioned into a $[Au_{11}]^{5+}$ core and two $[Au_5\{\mu\text{-}Fe(CO)_4\}_5]^{5-}$ rings containing linear Fe–Au–Fe motives (Fig. 28).[106,149] Similarly, $[Au_{25}(SCH_2CH_2Ph)_{18}]^-$ may be viewed as composed by a $[Au_{13}]^{5+}$ core and six $[Au_2(SR)_3]^-$ staple motives.

Häkkinen and Femoni have further analyzed these iron-carbonyl-protected gold clusters by near-infrared (NIR) and Raman spectroscopy in conjunction with linear-response time-dependent density functional theory (LR-TDDFT).[50] In particular, the analyses of $[Au_{21}Fe_{10}(CO)_{40}]^{5-}$ and $[Au_{22}Fe_{12}(CO)_{48}]^{6-}$ (Fig. 29) indicate that their bonding and electronic structures display some analogies to thiolate-monolayer-protected Au clusters, and the frontier orbitals responsible for their NIR absorption may be rationalized in the framework of the gold superatom model.

The species $[Au_{16}S\{Fe(CO)_4\}_4(IPr)_4]^{2+}$ (IPr = $C_3N_2H_2(C_6H_3{}^iPr_2)_2$) was obtained upon thermal decomposition of [Fe$(CO)_4(AuIPr)_2$] in DMSO.[150] It consists of a μ_{12}-S centered Au_{12}-cubeoctahedron, decorated on the surface by four μ_3-Fe$(CO)_4$ and four μ_3-AuIPr fragments, with pseudo-T_d symmetry (Fig. 30 and 31). Icosahedral Au_{13} and $Au_{12}M$ cages have been found in several ligand-protected molecular gold nanoclusters,[30,31,35,44,151,152] whereas the cubeoctahedral core is less

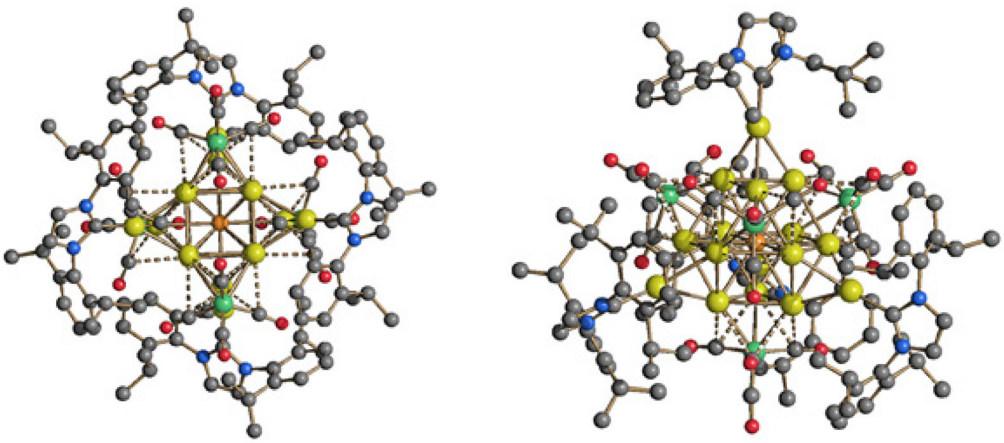

Fig. 30 Two different views of the molecular structure of $[Au_{16}S\{Fe(CO)_4\}_4(IPr)_4]^{2+}$ (IPr = $C_3N_2H_2(C_6H_3{}^iPr_2)_2$). Au–C(O) contacts [2.636(4)–2.723(4) Å] were represented as fragmented lines. Hydrogen atoms have been omitted (green Fe; yellow Au; orange S; blue N; red O; grey C). Adapted with permission from ref. 150 Copyright 2020 American Chemical Society.

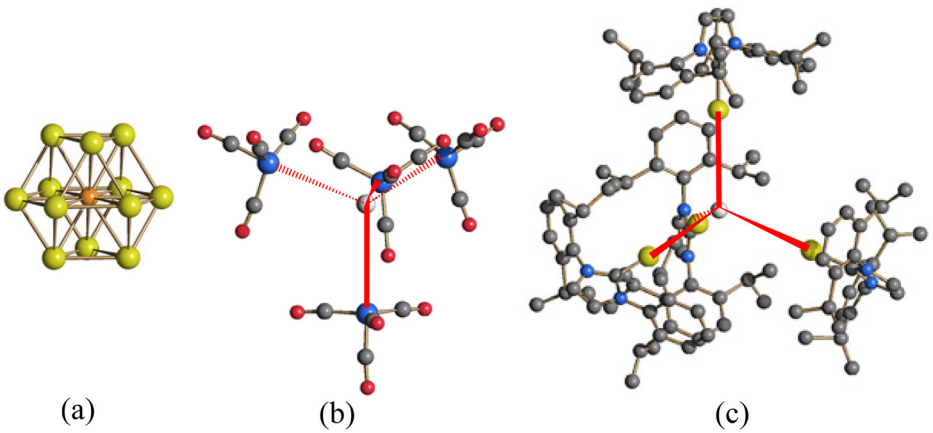

Fig. 31 Schematic representation of (a) the $Au_{12}S$ cubeoctahedral core of $[Au_{16}S\{Fe(CO)_4\}_4(IPr)_4]^{2+}$ (IPr = $C_3N_2H_2(C_6H_3{}^iPr_2)_2$), and the tetrahedral arrangements of (b) the four μ_3-Fe$(CO)_4$ groups and (c) the four μ_3-AuIPr fragments (green Fe; yellow Au; orange S; blue N; red O; grey C). The center of the cluster is represented as a white sphere in (b) and (c).

common.[153] The electron count of $[Au_{16}S\{Fe(CO)_4\}_4(IPr)_4]^{2+}$ can be derived assuming that the μ_3-AuIPr fragments, isolobal to μ_3-H, contribute one electron each, the μ_3-$Fe(CO)_4$ groups are four electron donors, and the interstitial μ_6-S atom donates six electrons.[150] Overall, $[Au_{16}S\{Fe(CO)_4\}_4(IPr)_4]^{2+}$ possesses 156 CVE [11 × 12 (Au) + 6 × 1 (μ_6-S) + 4 × 1 (μ_3-AuIPr) + 4 × 4 (μ_3-$Fe(CO)_4$) −2 (charge +2)]. According to the EAN (Effective Atomic Number) rule, a cubeoctahedron should have 168 CVE. PSEPT (Polyhedral Skeletal Electron Pair Theory) predicted 170 CVE by interpreting a cubeoctahedron as a four-connected polyhedron. Conversely, assuming that radial bonding predominates, on the basis of Mingos Rules a cubeoctahedron should have 162 CVE. In all cases, $[Au_{16}S\{Fe(CO)_4\}_4(IPr)_4]^{2+}$ results electron poor, as often found for gold clusters.

4. Conclusions

Two general types of molecular clusters may be classified as surface decorated MCCs. These include clusters composed of a metal carbonyl core decorated on the surface by ML fragments, as well as clusters composed of a naked metal core decorated and stabilized on the surface by metal-carbonyl fragments. All of these possess a metal core of various geometries stabilized upon coordination to its surfaces of different metal-ligands or metal-CO fragments. Most of the work appeared to date concerns the syntheses of surface decorated MCCs and their structural characterization by SC-XRD. Some of the most noticeable examples appeared in the literature have been reported in this Frontier Article, mainly outlining the contribution of our research group in Bologna to this field.

The examples herein reported show the rich structural and chemical diversity of surface decorated MCCs, as well as the possibility of obtained higher nuclearity clusters. Beside the aesthetical pleasure generated by these species, they allow to access unusual structural motives and geometries. At this regard, some structural analogies can be drawn among some of these surface decorated MCCs and other categories of ligated clusters, such as ligand protected coinage metal nanoclusters. In particular, the M-ligand and M–CO fragments decorating some of these surface decorated MCCs display some resemblances to the staple motives reported for ligand protected Au nanoclusters and related species. Moreover, the superatom model, usually applied to coinage metal nanoclusters, has been recently applied also to some representative examples of surface decorated MCCs.[50–53] Further structural and theoretical work will be required in order to fully explore the potentialities of these analogies, hopefully leading to a general unified approach for the interpretation of the different categories of molecular ligated metal clusters.

At this regard, it is noteworthy that, adopting the electron counting rules of low valent metal clusters (whose classically employed for MCCs), the surface decorated MCCs $[Pt_{13}(CO)_{12}\{Cd_5(\mu\text{-}Br)_5Br_2(dmf)_3\}_2]^{2-}$ and $[Pt_{13}\{Au_2(PPh_3)_2\}_2(CO)_{10}(PPh_3)_4]$, the Au-phosphine cluster $[Au_{13}Cl_2(PMe_2Ph)_{10}]^{3+}$, and the Au-thiolate cluster $[Au_{25}(SCH_2CH_2Ph)_{18}]^-$, all possess 162 CVE (see section 2.1).[106–109] As predicted by Mingos, this electron counting is consistent with an icosahedral M_{13} core where radial bonds predominate over tangential ones.[110,111] Applying the superatom model to the same four icosahedral clusters, they result to be superatom with 8 free electrons.[51] This apparent "abnormal" difference in the electron counting (162 *vs.* 8) is due to how and which electrons are counted in the two schemes. CVE rules add all the valence electrons of the cluster, without differentiating between core electrons and those used for binding the ligands. Moreover, also the d electrons of the transition metals are included, even if the question might be debated in the case of Au. Of course, the metal framework (M–M bonding) is due to a reduced number of electrons (as a function of geometry). Most electrons are used to bind ligands (σ and π interactions) or are inert low lying core electrons. Conversely, in the superatom model only the electrons responsible for M–M bonds are counted, and d electrons are excluded. After considering these two points, the two models perfectly agree for the above mentioned four icosahedral clusters. Somehow, they say the same thing, but in a different manner. It would be important to extend this theoretical comparison among different electron counting models to other molecular metal clusters, in order to better appreciate such analogies.

From a practical point of view, MCCs already found several applications in catalysis and electrocatalysis.[9,13,128,154–158] Enhanced molecular electrocatalysts might be obtained based on the electron sponge behavior of larger MCCs.[19,159] Paramagnetic MCCs could be exploited as single molecular magnets.[160] MCCs were employed as models in surface science, particularly for Fischer–Tropsch chemistry, and gave a fundamental contribution to the development of the cluster-surface analogy.[161,162] More recently, iron carbide MCCs garnered attention in bioinorganic chemistry, as spectroscopic, structural and functional models of the nitrogenase active site cluster.[163] Such studies require the partial replacement of carbonyls with other ligands, and the introduction of organic and inorganic sulfur based ligands is rather challenging.[164] CO-substitution may lead also to water-soluble MCCs, that might have potential biological and pharmaceutical applications.[165] Isomerism and chirality are two other fields of increasing interest in molecular cluster chemistry,[166,167] whose investigation in the case of MCCs is at its beginning.[168,169] New molecular materials integrated with MCCs can be obtained by self-assembly phenomena exploiting the formation of homometallic or heterometallic bonds, or employing suitable bidentate ligands.[11,18,101] Indeed, self-assembly can be exploited for the construction of cluster-based polymers for optoelectronics, magnetism, catalysis and nanotechnology.[11,170,171] A further strategy for the preparation of MCC based materials is represented by their encapsulation within metal organic framework (MOF),[172] affording nanostructures materials for potential applications in catalysis and electrocatalysis.[173] Finally, MCCs may be used as molecular precursors in controlled thermal processes for the synthesis of supported metal cata-

lysts, metal nanocrystals embedded in porous matrices, magnetic nanoalloys, and conductive sub-micrometric metal wires.[18,174–178]

Data availability

No primary research results, software, or code have been included and no new data were generated or analyzed as part of this Frontier Article.

Conflicts of interest

There are no conflicts to declare.

Acknowledgements

Financed by the European Union – NextGenerationEU through the Italian Ministry of University and Research under PNRR – Mission 4 Component 1, Investment 4.1 (DM 118/2023) – CUP J33C23002200002. We thank the referees for useful suggestions in revising the manuscript.

References

1 F. A. Cotton, Transition-metal compounds containing clusters of metal atoms, *Q. Rev., Chem. Soc.*, 1966, **20**, 389–401.
2 A. V. Virovets, E. Peresypkina and M. Scheer, Structural Chemistry of Giant Metal Based Supramolecules, *Chem. Rev.*, 2021, **121**, 14885–14554.
3 J. E. McGrady, F. Weigend and S. Dehnen, Electronic structure and bonding in endohedral Zintl clusters, *Chem. Soc. Rev.*, 2002, **51**, 628–649.
4 J. Heine, B. Peerless, S. Dehnen and C. Lichtenberg, Charge Makes a Difference: Molecular Ionic Bismuth Compounds, *Angew. Chem., Int. Ed.*, 2023, **62**, e202218771.
5 M. Schütz, C. Gemel, W. Klein, R. A. Fischer and T. F. Fässler, Intermetallic phases meet intermetalloid clusters, *Chem. Soc. Rev.*, 2021, **50**, 8496–8510.
6 J. Qian, Z. Yang, J. Lyu, Q. Yao and J. Xie, Molecular Interactions in Atomically Precise Metal Nanoclusters, *Precis. Chem.*, 2024, **2**, 495–517.
7 K. Wang, T. Iwano and S. Uchida, Keplerate polyoxometalate compounds: a multifunctional nano-platform for advanced materials, *Dalton Trans.*, 2024, **53**, 16797–16806.
8 E. L. Albright, T. I. Levchenko, V. K. Kulkarni, A. I. Sullivan, J. F. DeJesus, S. Malola, S. Takano, M. Nambo, K. Stamplecoskie, H. Häkkinen, T. Tsukuda and C. M. Crudden, *N*-Heterocyclic Carbene-Stabilized Atomically Precise Metal Nanoclusters, *J. Am. Chem. Soc.*, 2024, **146**, 5759–5780.
9 C. Cesari, J.-H. Shon, S. Zacchini and L. A. Berben, Metal carbonyl clusters of groups of 8–10: synthesis and catalysis, *Chem. Soc. Rev.*, 2021, **50**, 9503–9539.
10 P. R. Raithby, The growth of higher nuclearity carbonyl clusters of ruthenium and osmium, *J. Organomet. Chem.*, 2024, **1005**, 122979.
11 M. Shieh, Y.-H. Liu, Y.-H. Li and R. Y. Lin, Metal carbonyl cluster-based coordination polymers: diverse syntheses, versatile network structures, and special properties, *CrystEngComm*, 2019, **21**, 7341–7364.
12 E. G. Mednikov and L. F. Dahl, Syntheses, structures and properties of primarily nanosized homo/heterometallic palladium CO/PR_3-ligated clusters, *Philos. Trans. R. Soc., A*, 2010, **368**, 1301–1332.
13 C. Cesari, C. Femoni, F. Forti, M. C. Iapalucci, G. Scorzoni and S. Zacchini, Molecular hydride carbonyl clusters and nanoclusters, *Inorg. Chim. Acta*, 2025, **574**, 122394.
14 C. Cesari, C. Femoni, M. C. Iapalucci and S. Zacchini, Molecular Fe, Co and Ni carbide carbonyl clusters and nanoclusters, *Inorg. Chim. Acta*, 2023, **544**, 121235.
15 I. Ciabatti, C. Femoni, M. C. Iapalucci, S. Ruggieri and S. Zacchini, The role of gold in transition metal carbonyl clusters, *Coord. Chem. Rev.*, 2018, **355**, 27–38.
16 B. Berti, C. Femoni, M. C. Iapalucci, S. Ruggieri and S. Zacchini, Functionalization, Modification, and Transformation of Platinum Chini Clusters, *Eur. J. Inorg. Chem.*, 2018, 3285–3296.
17 I. Ciabatti, C. Femoni, M. C. Iapalucci, G. Longoni and S. Zacchini, Platinum Carbonyl Clusters Chemistry: Four Decades of Challenging Nanoscience, *J. Cluster Sci.*, 2014, **25**, 115–146.
18 S. Zacchini, Using Metal Carbonyl Clusters To Develop a Molecular Approach towards Metal Nanoparticles, *Eur. J. Inorg. Chem.*, 2011, 4125–4145.
19 C. Femoni, M. C. Iapalucci, F. Kaswalder, G. Longoni and S. Zacchini, The possible role of metal carbonyl clusters in nanoscience and nanotechnologies, *Coord. Chem. Rev.*, 2006, **250**, 1580–1604.
20 B. F. G. Johnson and S. McIndoe, Spectroscopic and mass spectrometric methods for the characterisation of metal clusters, *Coord. Chem. Rev.*, 2000, **200–202**, 901–932.
21 K. H. Whitmire, Transition metal complexes of the naked pnictide elements, *Coord. Chem. Rev.*, 2018, **376**, 114–195.
22 J. A. Cabeza and P. G. Álvarez, The N-heterocyclic carbene chemistry of transition-metal carbonyl clusters, *Chem. Soc. Rev.*, 2011, **40**, 5389–5405.
23 G. Hogarth, S. E. Kabir and E. Nordlander, Cluster chemistry in the Noughties: new developments and their relationship to nanoparticles, *Dalton Trans.*, 2010, **39**, 6153–6174.
24 M. Sellin and I. Krossing, Homoleptic Transition Metal Carbonyl Cations: Synthetic Approaches, Characterization and Follow-Up Chemistry, *Acc. Chem. Res.*, 2023, **56**, 2776–2787.
25 D. M. P. Mingos, Structural and bonding patterns in gold clusters, *Dalton Trans.*, 2015, **44**, 6680–6695.

26 M. L. Ganadu, F. Demartin, A. Panzanelli, E. Zangrando, M. Peana, S. Medici and M. A. Zoroddu, Gold Clusters: From the Dispute on a Gold Chair to the Golden Future of Nanostructures, *Molecules*, 2021, **26**, 5014.
27 L. Malatesta, Cluster compounds of gold, *Gold Bull.*, 1975, **8**, 48–52.
28 L. Naldini, F. Cariati, G. Simonetta and L. Malatesta, Gold-tertiary phosphine derivatives with intermetallic bonds, *Chem. Commun.*, 1966, 647–648.
29 L. Malatesta, L. Naldini, G. Simonetta and F. Cariati, Triphenylphosphine-gold(0)-gold(I) compounds, *Coord. Chem. Rev.*, 1966, **1**, 255–262.
30 R. Jin, C. Zeng, M. Zhou and Y. Chen, Atomically Precise Colloidal Metal Nanoclusters and Nanoparticles: Fundamentals and Opportunities, *Chem. Rev.*, 2016, **116**, 10346–10413.
31 I. Chakraborty and T. Pradeep, Atomically Precise Clusters of Noble Metals: Emerging Link between Atoms and Nanoparticles, *Chem. Rev.*, 2017, **117**, 8208–8271.
32 S. Li, N.-N. Li, X.-Y. Dong, S.-Q. Zang and T. C. W. Mak, Chemical Flexibility of Atomically Precise Metal Clusters, *Chem. Rev.*, 2024, **124**, 7262–7378.
33 X. Zou, X. Kang and M. Zhu, Recent developments in the investigation of driving forces for transforming coinage metal nanoclusters, *Chem. Soc. Rev.*, 2023, **52**, 5892–5967.
34 M. F. Matus and H. Häkkinen, Understanding ligand-protected noble metal nanoclusters at work, *Nat. Rev. Mater.*, 2023, **8**, 372–389.
35 W. W. Xu, X. C. Zeng and Y. Gao, The structural isomerism in gold nanoclusters, *Nanoscale*, 2018, **10**, 9476–9483.
36 C. Sun, B. K. Teo, C. Deng, J. Lin, G.-G. Luo, C.-H. Tung and D. Sun, Hydrido-coinage-metal-clusters: Rational design, synthetic protocols and structural characteristics, *Coord. Chem. Rev.*, 2021, **427**, 213576.
37 T.-H. Chiu, J.-H. Liao, R. P. B. Silalahi, M. N. Pillay and C. W. Liu, Hydride-doped coinage metal superatom and their catalytic applications, *Nanoscale Horiz.*, 2024, **9**, 675–692.
38 X. Kang, Y. Li, M. Zhu and R. Jin, Atomically precise alloy nanoclusters: syntheses, structures, and properties, *Chem. Soc. Rev.*, 2020, **49**, 6443–6514.
39 T. Kawawaki, T. Okada, D. Hirayama and Y. Negishi, Atomically precise metal nanoclusters as catalysts for electrocatalytic CO_2 reduction, *Green Chem.*, 2024, **26**, 122–163.
40 R. Jin, G. Li, S. Sharma, Y. Li and X. Du, Toward Active-Site Tailoring in Heterogeneous Catalysis by Atomically Precise Metal Nanoclusters with Crystallographic Structures, *Chem. Rev.*, 2021, **121**, 567–648.
41 N. D. Loewen, T. V. Neelakantan and L. A. Berben, Renewable Formate from C-H Bond Formation with CO_2: Using Iron Carbonyl Clusters as Electrocatalysts, *Acc. Chem. Res.*, 2017, **50**, 2362–2370.
42 S. Mai, J. Sun, Z. Fang, G.-B. Xiao and J. Cao, Metal Clusters Based Multifunctional Materials for Solar Cells, *Chem. – Eur. J.*, 2024, **30**, e202303973.
43 F. Zaera, Designing Sites in Heterogeneous Catalysis: Are We Reaching Selectivities Competitive With Those of Homogeneous Catalysis?, *Chem. Rev.*, 2022, **122**, 8594–8757.
44 P. D. Jadzinsky, G. Calero, C. J. Ackerson, D. A. Bushnell and R. D. Kornberg, Structure of a Thiol Monolayer-Protected Gold Nanoparticle at 1.1 Å Resolution, *Science*, 2007, **318**, 430–433.
45 H. Häkkinen, The gold-sulfur interface at the nanoscale, *Nat. Chem.*, 2012, **4**, 443–455.
46 S. M. Owen, Electron counting in clusters: a view of the concepts, *Polyhedron*, 1988, **7**, 253–283.
47 W. W. Xu, X. C. Zeng and Y. Gao, Application of Electronic Counting Rules for Ligand-Protected Gold Nanoclusters, *Acc. Chem. Res.*, 2018, **51**, 2739–2747.
48 H. Häkkinen, Atomic and electronic structure of gold clusters: understanding flakes, cages and superatoms from simple concepts, *Chem. Soc. Rev.*, 2008, **37**, 1847–1859.
49 C. M. Aikens, R. Jin, X. Roy and T. Tsukuda, From atom-precise nanoclusters to superatom materials, *J. Chem. Phys.*, 2022, **156**, 170401.
50 O. Lopez-Acevedo, J. Rintala, S. Virtanen, C. Femoni, C. Tiozzo, H. Grönbeck, M. Pettersson and H. Häkkinen, Characterization of Iron-Carbonyl Protected Gold Clusters, *J. Am. Chem. Soc.*, 2009, **131**, 12573–12575.
51 J. Wei, R. Marchal, D. Astruc, S. Kahlal, J.-F. Halet and J.-Y. Saillard, Looking at platinum carbonyl nanoclusters as *superatoms*, *Nanoscale*, 2022, **14**, 3946–3957.
52 W. Unkrig, K. Kloiber, B. Butschke, D. Kratzert and I. Krossing, Altering Charges on Heterobimetallic Transition-Metal Carbonyl Clusters, *Chem. – Eur. J.*, 2020, **26**, 12373–12381.
53 A. Muñoz-Castro, sp^3-hybridization in superatomic clusters. Analogues to simple molecules involving the Au_6 core, *Chem. Sci.*, 2014, **5**, 4749–4754.
54 J. W. Lauher and K. Wald, Synthesis and Structure of $[FeCo_3(CO)_{12}AuPPh_3]$: A Trimetallic Trigonal-Bipyramidal Cluster. Gold Derivatives as Structural Analogues of Hydrides, *J. Am. Chem. Soc.*, 1981, **103**, 7648–7650.
55 P. Braunstein, J. Rosé, Y. Dusausoy and J.-P. Mangeot, Complexes à liaisons métal-métal. XXI. Synthèse et structure du "cluster" $(Ph_3P)AuRuCo_3(CO)_{12}$: une bipyramide trigonale à trois métaux différents, *C. R. Chim.*, 1982, **294**, 967–970.
56 P. Braunstein and J. Rosé, Gold in Bimetallic Molecular Clusters. Their Synthesis, Bonding and Catalytic Reactivities, *Gold Bull.*, 1985, **18**, 17–30.
57 P. Braunstein, H. Lehner, D. Matt, A. Tiripicchio and M. Tiripicchio-Camellini, Synthesis of the first Pt-Au cluster by an unexpected H^+-substitution at trans-PtH(Cl)L_2, *Angew. Chem., Int. Ed. Engl.*, 1984, **23**, 304–304.
58 S. Sculfort and P. Braunstein, Intramolecular d^{10}-d^{10} interactions in heterometallic clusters of the transition metals, *Chem. Soc. Rev.*, 2011, **40**, 2741–2760.
59 H. Schmidbaur and A. Schier, Aurophilic interactions as a subject of current research: an up-date, *Chem. Soc. Rev.*, 2012, **41**, 370–412.

60 P. Pyykkö, Strong closed-shell interactions in inorganic chemistry, *Chem. Rev.*, 1997, **97**, 597–636.
61 A. Das, U. Das and A. K. Das, Relativistic effects on the chemical bonding properties of the heavier elements and their compounds, *Coord. Chem. Rev.*, 2023, **479**, 215000.
62 N. Mirzadeh, H. Privér, A. J. Blake and H. Schmidbaur, Innovative Molecular Design Strategies in Materials Science Following the Aurophilicity Concept, *Chem. Rev.*, 2020, **120**, 7551–7591.
63 C. Cesari, B. Berti, F. Calcagno, C. Femoni, M. Garavelli, M. C. Iapalucci, I. Rivalta and S. Zacchini, Polymerization isomerism in Co-M (M = Cu, Ag, Au) carbonyl clusters: synthesis, structures and computational investigation, *Molecules*, 2021, **26**, 1529.
64 I. Ciabatti, C. Femoni, M. Hayatifar, M. C. Iapalucci, A. Ienco, G. Longoni, G. Manca and S. Zacchini, Octahedral Co-Carbide Carbonyl Clusters Decorated by $[AuPPh_3]^+$ Fragments: Synthesis, Structural Isomerism, and Aurophilic Interactions of $Co_6C(CO)_{12}(AuPPh_3)_4$, *Inorg. Chem.*, 2014, **53**, 9761–9770.
65 C. Cesari, M. Bortoluzzi, C. Femoni, F. Forti, M. C. Iapalucci and S. Zacchini, Peraurated ruthenium hydride carbonyl clusters: aurophilicity, isolobal analogy, structural isomerism, and fluxionality, *Dalton Trans.*, 2024, **53**, 3865–3879.
66 M. Bortoluzzi, I. Ciabatti, C. Femoni, M. Hayatifar, M. C. Iapalucci, G. Longoni and S. Zacchini, Hydride Migration from a Triangular Face to a Tetrahedral Cavity in Tetranuclear Iron Carbonyl Clusters upon Coordination of $[AuPPh_3]^+$ Fragments, *Angew. Chem., Int. Ed.*, 2014, **53**, 7233–7237.
67 M. Bortoluzzi, I. Ciabatti, C. Cesari, C. Femoni, M. C. Iapalucci and S. Zacchini, Synthesis of the highly reduced $[Fe_6C(CO)_{15}]^{4-}$ carbonyl carbide cluster and its reactions with H^+ and $[Au(PPh_3)]^+$, *Eur. J. Inorg. Chem.*, 2017, 3135–3143.
68 I. Ciabatti, C. Femoni, M. Hayatifar, M. C. Iapalucci and S. Zacchini, Co_5C and Co_4C carbido carbonyl clusters stabilized by $[AuPPh_3]^+$ fragments, *Inorg. Chim. Acta*, 2015, **428**, 203–211.
69 I. Ciabatti, C. Femoni, M. C. Iapalucci, A. Ienco, G. Longoni, G. Manca and S. Zacchini, Intramolecular d^{10}-d^{10} Interactions in a $Ni_6C(CO)_9(AuPPh_3)_4$ Bimetallic Nickel-Gold carbide Carbonyl Cluster, *Inorg. Chem.*, 2013, **52**, 10559–10565.
70 M. Bortoluzzi, I. Ciabatti, C. Femoni, M. Hayatifar, M. C. Iapalucci, G. Longoni and S. Zacchini, Peraurated nickel carbide carbonyl clusters: the cationic $[Ni_6(C)(CO)_8(AuPPh_3)_8]^{2+}$ monocarbide and the $[Ni_{12}(CO)(C_2)(CO)_{17}(AuPPh_3)_3]^-$ anion containing one carbide and one acetylide unit, *Dalton Trans.*, 2014, **43**, 13471–13475.
71 A. Ceriotti, P. Macchi, A. Sironi, S. El Afefey, M. Daghetta, S. Fedi, F. Fabrizi de Biani and R. Della Pergola, Cooperative Effects of Electron Donors and Acceptors for the Stabilization of Elusive Metal Cluster Frameworks: Synthesis and Solid-State Structures of $[Pt_{19}(CO)_{24}(\mu_4\text{-}AuPPh_3)_3]^-$ and $[Pt_{19}(CO)_{24}\{\mu_4\text{-}Au_2(PPh_3)_2\}_2]$, *Inorg. Chem.*, 2013, **52**, 1960–1964.
72 V. Dearing, S. R. Drake, B. F. G. Johnson, J. Lewis, M. McPartlin and H. R. Powell, The synthesis of the first tetra- and penta-gold decaosmium clusters, X-ray structure analysis of $[Os_{10}Au_4C(CO)_{24}\{P(C_6H_{11})_3\}_3]$, *J. Chem. Soc., Chem. Commun.*, 1988, 1331–1333.
73 M. Bortoluzzi, C. Cesari, I. Ciabatti, C. Femoni, M. Hayatifar, M. C. Iapalucci, R. Mazzoni and S. Zacchini, Bimetallic Fe-Au Carbonyl Clusters Derived from Collman's Reagent: Synthesis, Structure and DFT Analysis of $Fe(CO)_4(AuNHC))_2$ and $[Au_3Fe_2(CO)_8(NHC)_2]^-$, *J. Cluster Sci.*, 2017, **28**, 703–723.
74 R. Della Pergola, A. Sironi, A. Rosehr, V. Colombo and A. Sironi, N-heterocyclic carbene copper complexes tethered to iron carbidocarbonyl clusters, *Inorg. Chem. Commun.*, 2014, **49**, 27–29.
75 R. D. Adams, J. Tedder and Y. O. Wong, Phenyl-gold complexes of Ru_6 and Ru_5 carbonyl clusters, *J. Organomet. Chem.*, 2015, **795**, 2–10.
76 C.-N. Lin, C.-Y. Huang, C.-C. Yu, Y.-M. Chen, W.-M.- Ke, G.-J. Wang, G.-A. Lee and M. Shieh, Iron carbonyl cluster-incorporated Cu(I) NHC complexes in homocoupling of arylboronic acids: an effective $[TeFe_3(CO)_9]^{2-}$ ligand, *Dalton Trans.*, 2015, **44**, 16675–16679.
77 M. K. Karunananda, S. R. Parmelee, G. W. Waldhart and N. P. Mankad, Experimental and Computational Characterization of the Transition State for C-X Bimetallic Oxidative Addition at a Cu-Fe Reaction Center, *Organometallics*, 2015, **34**, 3857–3864.
78 R. D. Adams and G. Elpitiya, The addition of Gold and Tin to Bismuth-Triiridium Carbonyl Complexes, *Inorg. Chem.*, 2015, **54**, 8042–8048.
79 R. D. Adams, P. Dhull, V. Rassolov and Y. O. Wong, Synthesis and Reactivity of Electronically Unsaturated Dirhenium Carbonyl Compounds Containing Bridging Gold-Carbene Groups, *Inorg. Chem.*, 2016, **55**, 10475–10483.
80 B. Berti, M. Bortoluzzi, C. Cesari, C. Femoni, M. C. Iapalucci, R. Mazzoni, F. Vacca and S. Zacchini, Synthesis and Characterization of Heterobimetallic Carbonyl Clusters with Direct Au-Fe and Au···Au Interactions Supported by *N*-Heterocyclic Carbene and Phosphine Ligands, *Eur. J. Inorg. Chem.*, 2019, 3084–3093.
81 B. Berti, M. Bortoluzzi, C. Cesari, C. Femoni, M. C. Iapalucci, R. Mazzoni and S. Zacchini, A Comparative Experimental and Computational Study of Heterometallic Fe-M (M = Cu, Ag, Au) Carbonyl Clusters Containing N-Hetericyclic Carbene Ligands, *Eur. J. Inorg. Chem.*, 2020, 2191–2202.
82 C. Cesari, B. Berti, F. Calcagno, C. Lucarelli, M. Garavelli, R. Mazzoni, I. Rivalta and S. Zacchini, Bimetallic Co-M (M = Cu, Ag, and Au) Carbonyl Complexes Supported by *N*-Heterocyclic Carbene Ligands: Synthesis, Structures, Computational Investigation, and Catalysis for Ammonia

Borane Dehydrogenation, *Organometallics*, 2021, **40**, 2724–2735.

83 M. Bortoluzzi, C. Cesari, I. Ciabatti, C. Femoni, M. C. Iapalucci and S. Zacchini, Reactions of Platinum Carbonyl Chini Clusters with Ag(NHC)Cl Complexes: Formation of Acid-Base Lewis Adducts and Heteroleptic Clusters, *Inorg. Chem.*, 2017, **56**, 6532–6544.

84 C. Cesari, I. Ciabatti, C. Femoni, M. C. Iapalucci and S. Zacchini, Capping $[H_{8-n}Ni_{42}C_8(CO)_{44}]^{n-}$ (n = 6, 7, 8) Octa-carbide Carbonyl Nanoclusters with [Ni(CO)] and [CuCl] Fragments, *J. Cluster Sci.*, 2017, **28**, 1963–1979.

85 A. Bernardi, I. Ciabatti, C. Femoni, M. C. Iapalucci, G. Longoni and S. Zacchini, Molecular nickel poly-carbide carbonyl nanoclusters: The octa-carbide $[HNi_{42}C_8(CO)_{44}(CuCl)]^{7-}$ and the deca-carbide $[Ni_{45}C_{10}(CO)_{46}]^{6-}$, *J. Organomet. Chem.*, 2016, **812**, 229–239.

86 A. Bernardi, I. Ciabatti, C. Femoni, M. C. Iapalucci, G. Longoni and S. Zacchini, Ni-Cu tetracarbide carbonyls with vacant Ni(CO) fragments as borderline compounds between molecular and quasi-molecular clusters, *Dalton Trans.*, 2013, **42**, 407–421.

87 A. Bernardi, C. Femoni, M. C. Iapalucci, G. Longoni, F. Ranuzzi, S. Zacchini, P. Zanello and S. Fedi, Synthesis, Molecular Structure and Properties of the $[H_{6-n}Ni_{30}C_4(CO)_{34}(CdCl)_2]^{n-}$ (n = 3–6) Bimetallic Carbide Carbonyl Cluster: A Model for the Growth of Noncompact Interstitial Metal Carbides, *Chem. – Eur. J.*, 2008, **14**, 1924–1934.

88 A. Bernardi, C. Femoni, M. C. Iapalucci, G. Longoni and S. Zacchini, Cadmium-substitution promoted by nucleophilic attack of $[Ni_{30}C_4(CO)_{34}(CdX)_2]^{6-}$ (X = Cl, Br, I) carbide carbonyl clusters: Synthesis and characterization of the new $[H_{7-n}Ni_{32}C_4(CO)_{36}(CdX)]^{n-}$ (X = Cl, Br, I; n = 5, 6, 7), *Inorg. Chim. Acta*, 2009, **362**, 1239–1246.

89 A. Bernardi, C. Femoni, M. C. Iapalucci, G. Longoni, S. Zacchini, S. Fedi and P. Zanello, Synthesis, Structures and Electrochemistry of New Carbonylnickel Octacarbide Clusters: The Distorting Action of Carbide Atoms in the Growth of Ni Cages and the First Example of the Inclusion of a Carbon Atom within a (Distorted) Ni Octahedral Cage, *Eur. J. Inorg. Chem.*, 2010, 4831–4842.

90 C. Capacci, C. Cesari, C. Femoni, M. C. Iapalucci, F. Mancini, S. Ruggieri and S. Zacchini, Structural Diversity in Molecular Nickel Phosphide Carbonyl Nanoclusters, *Inorg. Chem.*, 2020, **59**, 16016–16026.

91 C. Femoni, M. C. Iapalucci, G. Longoni, S. Zacchini, S. Fedi and F. Fabrizi de Biani, Nickel poly-acetylide carbonyl clusters: structural features, bonding and electrochemical behaviour, *Dalton Trans.*, 2012, **41**, 4649–4663.

92 R. D. Adams, B. Captain, W. Fu, P. J. Pellechia and M. D. Smith, Remarkable Dynamical Opening and Closing of Platinum and Palladium Pentaruthenium Carbido Carbonyl Cluster Complexes, *Inorg. Chem.*, 2003, **42**, 2094–2101.

93 R. D. Adams, B. Captain, W. Fu and M. D. Smith, Lewis Acid-Base Interactions between Metal Atoms and Their Applications for the Synthesis of Bimetallic Cluster Complexes, *J. Am. Chem. Soc.*, 2002, **124**, 5628–5629.

94 S. Saha and B. Captain, Synthesis and Structural Characterization of Ruthenium Carbonyl Cluster Complexes Containing Platinum with a Bulky N-Heterocyclic Carbene Ligand, *Inorg. Chem.*, 2014, **21**, 1210–1216.

95 R. D. Adams and B. Captain, Unusual Structures and Reactivity of Mixed Metal Cluster Complexes Containing the Palladium/Platinum Tri-*t*-butylphosphine Grouping, *Acc. Chem. Res.*, 2009, **42**, 409–418.

96 A. Koppaka, V. Zollo Jr., S. Etezadi, D. C. Lever and B. Captain, Addition of Pt(IPr) Groupings to Ru_5 Carbide Gives New Mixed-Metal Pt-Ru Cluster Complexes, *J. Cluster Sci.*, 2016, **27**, 1671–1681.

97 M. Kawano, J. W. Bacon, C. F. Campana, B. E. Winger, J. D. Dudek, S. A. Sirchio, S. L. Scruggs, U. Geiser and L. F. Dahl, High-Nuclearity Close-Packed Palladium-Nickel Carbonyl Phosphine Clusters: Heteropalladium $[Pd_{16}Ni_4(CO)_{22}(PPh_3)_4]^{2-}$ and $[Pd_{33}Ni_9(CO)_{41}(PPh_3)_6]^{4-}$ Containing Pseudo-T_d ccp $Pd_{16}Ni_4$ and Pseudo-D_{3h} hcp $Pd_{33}Ni_9$ Cages, *Inorg. Chem.*, 2001, **40**, 2554–2569.

98 J. D. Erickson, E. G. Mednikov, S. A. Ivanov and L. F. Dahl, Isolation and Structural Characterization of a Makay 55-Metal-Atom Two-Shell Icosahedron of Pseudo-I_h Symmetry, $Pd_{55}L_{12}(\mu_3\text{-}CO)_{20}$ (L = PR_3, R = isopropyl): Comparative Analysis with Interior Two-Shell Icosahedral Geometries in Capped Three-Shell Pd_{145}, Pt-Centered Four-Shell Pd-Pt M_{165}, and Four-Shell Au_{133} Nanoclusters, *J. Am. Chem. Soc.*, 2016, **138**, 1502–1505.

99 M. Bortoluzzi, I. Ciabatti, C. Femoni, M. Hayatifar, M. C. Iapalucci and S. Zacchini, $[H_{3-n}Fe_4(CO)_{12}(IrCOD)]^{n-}$ (n = 1, 2) and $[H_2Fe_3(CO)_{10}(IrCOD)]^-$ Bimetallic Fe-Ir Hydride Carbonyl Clusters, *Organometallics*, 2015, **34**, 189–197.

100 F. Forti, C. Cesari, M. Bortoluzzi, C. Femoni, T. Funaioli, M. C. Iapalucci and S. Zacchini, Heterometallic Ru-Ir hydride carbonyl clusters, *J. Cluster Sci.*, 2025, **36**, 6.

101 C. Femoni, F. Kaswalder, M. C. Iapalucci, G. Longoni and S. Zacchini, Copolymerization of Pt-carbonyl clusters with Lewis acids: synthesis and crystal structure of the molecular $\{Cd_2Cl_4[Pt_9(CO)_{18}]^{2-}\}_($ 1-D polymer, *Chem. Commun.*, 2006, 2135–2137.

102 A. Bernardi, C. Femoni, M. C. Iapalucci, G. Longoni and S. Zacchini, The problems of detecting hydrides in metal carbonyl clusters by ^{1}H NMR: the case study of $[H_{4-n}Ni_{22}(C_2)_4(CO)_{28}(CdBr)_2]^{n-}$ (n = 2–4), *Dalton Trans.*, 2009, 4245–4251.

103 C.-Y. Miu, H.-H. Chi, S.-W. Chen, J.-J. Cherng, M.-H. Hsu, Y.-X. Huang and M. Shieh, Reactions of the μ_3-sulfido triiron cluster $[SFe_3(CO)_9]^{2-}$ with functionalized organic halides and mercury salts: selective reactivity, electrochemistry, and theoretical calculations, *New J. Chem.*, 2011, **35**, 2442–2455.

104 U. Brand and J. R. Shapley, Carbidohexarhenate Cluster Cores Bicapped by Mercury with Acetate or Thiolate Ligands, *Inorg. Chem.*, 2000, **39**, 32–36.

105 C. A. Wright and J. R. Shapley, Carbidoheptarhenate Cluster Complexes of Cadmium and Zinc Units: The Structure of $[PPh_4]_2[Re_7C(CO)_{21}(\mu_3\text{-ZnCl})]$, *Inorg. Chem.*, 2001, **40**, 6338–6340.

106 C. Femoni, M. C. Iapalucci, G. Longoni, S. Zacchini and S. Zarra, Icosahedral Pt-Centered Pt_{13} and Pt_{19} Carbonyl Clusters Decorated by $[Cd_5(\mu\text{-Br})_5Br_{5-x}(solvent)_x]^{x+}$ Rings Reminiscent of the Decoration of Au-Fe-CO and Au-Thiolate Nanoclusters: A Unifying Approach to Their Electron Counts, *J. Am. Chem. Soc.*, 2011, **133**, 2406–2409.

107 I. Ciabatti, C. Femoni, M. C. Iapalucci, G. Longoni, S. Zacchini and S. Zarra, Surface decorated platinum carbonyl clusters, *Nanoscale*, 2012, **4**, 4166–4177.

108 J.-F. Halet, D. G. Evans and D. M. P. Mingos, Effect of Cavity Size on the Charge Distribution in Carbido-Metal Carbonyl Clusters and Its Possible Catalytic Implications, *J. Am. Chem. Soc.*, 1988, **110**, 87–90.

109 C. E. Briant, B. R. C. Theobald, J. W. White, L. K. Bell, D. M. P. Mingos and A. J. Welch, Synthesis and X-ray structural characterization of the centred icosahedral gold cluster compound $[Au_{13}(PMe_2Ph)_{10}Cl_2](PF_6)_3$; the realization of a theoretical prediction, *J. Chem. Soc., Chem. Commun.*, 1981, 201–202.

110 D. M. P. Mingos, Theoretical analyses and electron counting rules for high nuclearity clusters, *J. Chem. Soc., Chem. Commun.*, 1985, 1352–1354.

111 M. P. Johansson and P. Pyykkö, $WAu_{12}(CO)_{12}$?, *Chem. Commun.*, 2010, **46**, 3762–3764.

112 N. de Silva and L. F. Dahl, Synthesis and Structural Analysis of the First nanosized Platinum-Gold Carbonyl/Phosphine Cluster, $Pt_{13}[Au_2(PPh_3)_2]_2(CO)_{10}(PPh_3)_4$, Containing a Pt-Centered $[Ph_3Pau\text{-}AuPPh_3]$-Capped Icosahedral Pt_{12} Cage, *Inorg. Chem.*, 2005, **44**, 9604–9606.

113 F. Demartin, M. C. Iapalucci and G. Longoni, Synthesis and Characterization of Novel Types of Adducts of Nickel Carbonyl Clusters with Indium Halides: X-ray Structures of $[NEt_4]_3[Ni_6(\mu_3\text{-}InBr_3)(\eta^2\text{-}\mu_6\text{-}In_2Br_5)(CO)_{11}]\cdot Me_2CO$, $[NEt_4]_4[Ni_6(\eta^2\text{-}\mu_6\text{-}In_2Br_5)_2(CO)_{10}]\cdot Me_2CO$, and $[NEt_4]_4[Ni_{12}(\mu_6\text{-}In)(\eta^2\text{-}\mu_6\text{-}In_2Br_4OH)(CO)_{22}]$, *Inorg. Chem.*, 1993, **32**, 5536–5543.

114 B. Berti, M. Bortoluzzi, C. Cesari, C. Femoni, M. C. Iapalucci and S. Zacchini, Reactions of $[Pt_6(CO)_6(SnX_2)_2(SnX_3)_4]^{4-}$ (X = Cl, Br) with Acids: Syntheses and molecular structures of $[Pt_{12}(CO)_{10}(SnCl)_2(SnCl_2)_4\{Cl_2Sn(\mu\text{-}OH)SnCl_2\}_2]^{2-}$ And $[Pt_7(CO)_6(SnBr_2)_4\{Br_2Sn(\mu\text{-}OH)SnBr_2\}\{Br_2Sn(\mu\text{-}Br)SnBr_2\}]^{2-}$ Platinum carbonyl clusters decorated by Sn(II)-Fragments, *Inorg. Chim. Acta*, 2020, **503**, 119432.

115 M. Bortoluzzi, A. Ceriotti, I. Ciabatti, R. Della Pergola, C. Femoni, M. C. Iapalucci, A. Storione and S. Zacchini, Platinum carbonyl clusters stabilized by Sn(II)-based fragments: syntheses and structures of $[Pt_6(CO)_6(SnCl_2)_2(SnCl_3)_4]^{4-}$, $[Pt_9(CO)_8(SnCl_2)_3(SnCl_3)_2(Cl_2SnOCOSnCl_2)]^{4-}$ and $[Pt_{10}(CO)_{14}\{Cl_2Sn(OH)SnCl_2\}_2]^{2-}$, *Dalton Trans.*, 2016, **45**, 5001–5013.

116 M. Bortoluzzi, A. Ceriotti, C. Cesari, I. Ciabatti, R. Della Pergola, C. Femoni, M. C. Iapalucci, A. Storione and S. Zacchini, Syntheses of $[Pt_6(CO)_8(SnCl_2)(SnCl_3)_4]^{4-}$ and $[Pt_6(CO)_8(SnCl_2)(SnCl_3)_2(PPh_3)_2]^{2-}$ Platinum-Carbonyl Clusters Decorated by SnII Fragments, *Eur. J. Inorg. Chem.*, 2016, 3929–3949.

117 E. Brivio, A. Ceriotti, L. Garlaschelli, M. Manassero and M. Sansoni, Coordination of $SnCl_2$ and $GeCl_2$ onto a one dimensional platinum network: synthesis and structural characterization of the $[PPh_4]_2[Pt_8(ECl_2)_4(CO)_{10}]$ (E = Sn, Ge) complexes, *J. Chem. Soc., Chem. Commun.*, 1995, 2055–2056.

118 S. Saha, D. Isrow and B. Captain, Build-up of a Ru_6 octahedral cluster core stabilized by *tert*-butyl germyl ligands, *J. Organomet. Chem.*, 2014, **751**, 815–820.

119 A. B. Hungria, R. Raja, R. D. Adams, B. Captain, J. M. Thomas, P. A. Midgley, V. Golovko and B. F. G. Johnson, Single-Step Conversion of Dimethyl Terephthalate into Cyclohexanedimethanol with Ru_5PtSn, a Trimetallic Nanoparticle Catalyst, *Angew. Chem., Int. Ed.*, 2006, **45**, 4782–4785.

120 R. D. Adams, B. Captain and W. Fu, Facile introduction of bridging MPh_2 groups (M = Ge, Sn, Pb) into platinum-pentaruthenium and hexaruthenium carbide carbonyl cluster complexes, *J. Organomet. Chem.*, 2003, **671**, 158–165.

121 E. V. Grachova, P. Jutzi, B. Neumann, L. O. Schebaum, H.-G. Stammler and S. P. Tunik, Unusual selective substitution of triply bridging carbonyl ligands for GaCp* in $Rh_6(CO)_{16}$. Synthesis and structural characterization of the $Rh_6(\mu_3\text{-}CO)_{4-x}(\mu_3\text{-}GaCp^*)_x(CO)_{12}$ clusters, x = 1–4, *J. Chem. Soc., Dalton Trans.*, 2002, 302–304.

122 E. V. Grachova and G. Linti, Reactivity of InCp* Towards Transition Metal Carbonyl Clusters: Synthesis and Structural Characterization of the $Rh_6(CO)_{16-x}(InCp^*)_x$ Mixed-Metal Cluster Compounds, x = 1–2, *Eur. J. Inorg. Chem.*, 2007, 3561–3564.

123 P. Jutzi, B. Neumann, G. Reunmann and H.-G. Stammler, *Organometallics*, 1998, **17**, 1305–1314.

124 M. Bortoluzzi, I. Ciabatti, C. Femoni, T. Funaioli, M. Hayatifar, M. C. Iapalucci, G. Longoni and S. Zacchini, Homoleptic and heteroleptic Au(I) complexes containing the new $[Co_5C(CO)_{12}]^-$ cluster as ligand, *Dalton Trans.*, 2014, **43**, 9633–9646.

125 I. Ciabatti, C. Femoni, M. C. Iapalucci, G. Longoni, S. Zacchini, S. Fedi and F. Fabrizi de Biani, Syntehsis, Structure, and Electrochemsitry of the Ni-Au Carbonyl Cluster $[Ni_{12}Au(CO)_{24}]^{3-}$ and Its Relation to $[Ni_{32}Au_6(CO)_{44}]^{6-}$, *Inorg. Chem.*, 2012, **51**, 11753–11761.

126 G. Manca, F. Fabrizi de Biani, M. Corsini, C. Cesari, C. Femoni, M. C. Iapalucci, S. Zacchini and A. Ienco, Inverted Ligand Field in a Pentanuclear Bow Tie Au/Fe Carbonyl Cluster, *Inorg. Chem.*, 2022, **61**, 3484–3492.

127 S. Pan, S. M. N. V. T. Gorantla, D. Parasar, H. V. R. Dias and G. Frenking, Chemical Bonding in Homoleptic Carbonyl Cations $[M\{Fe(CO)_5\}_2]^+$ (M = Cu, Ag, Au), *Chem. – Eur. J.*, 2021, **27**, 6936–6944.

128 C. Cesari, M. Bortoluzzi, F. Forti, L. Gubbels, C. Femoni, M. C. Iapalucci and S. Zacchini, 2-D Molecular Alloy Ru-M (M = Cu, Ag, and Au) Carbonyl Clusters: Synthesis, Molecular Structure, Catalysis, and Computational Studies, *Inorg. Chem.*, 2022, **61**, 14726–14741.

129 H. Egold, M. Schraa, U. Flörke and J. Partyka, Synthesis of Novel Mixed Metal Cluster Complexes of Osmium and Mercury: Formation of the Wheel-Shaped Cluster Complexes $Os_6(\mu_6\text{-}Hg)(\mu\text{-}PR_2)_2(CO)_{20}$ (R = Ph, *i*-Bu), *Organometallics*, 2002, **21**, 1925–1932.

130 C. Cesari, M. Bortoluzzi, C. Femoni, M. C. Iapalucci and S. Zacchini, Mercurophilic interactions in heterometallic Ru-Hg carbonyl clusters, *Inorg. Chim. Acta*, 2023, **545**, 121281.

131 M. Fajardo, H. D. Holden, B. F. G. Johnson, J. Lewis and P. R. Raithby, Syntehsis and structural characterisation of the heteronuclear raft complex $[Os_3(CO)_{11}Hg]_3$, *J. Chem. Soc., Chem. Commun.*, 1984, 24–25.

132 L. H. Gade, B. F. G. Johnson, J. Lewis, M. McPartlin, T. Kotch and A. J. Lee, Photochemical Core Manipulation in High-Nuclearity Os-Hg Clusters, *J. Am. Chem. Soc.*, 1991, **113**, 8698–8704.

133 B. Berti, M. Bortoluzzi, C. Cesari, C. Femoni, M. C. Iapalucci, R. Mazzoni, F. Vacca and S. Zacchini, Polymerization Isomerism in $[\{MFe(CO)_4\}_n]^{n-}$ (M = Cu, Ag, Au; N = 3, 4) Molecular Clusters Supported by Metallophilic Interactions, *Inorg. Chem.*, 2019, **58**, 2911–2915.

134 P. Croizat, S. Sculfort, R. Welter and P. Braunstein, Hexa- and Octanuclear Heterometallic Clusters with Copper-, Silver-, or Gold-Molybdenum Bonds and d^{10}-d^{10} Interactions, *Organometallics*, 2016, **35**, 3949–3958.

135 N. Masciocchi, P. Cairati, F. Ragaini and A. Sironi, Ab initio XPRD structure determination of metal carbonyl clusters: the case of $[HgRu(CO)_4]_4$, *Organometallics*, 1993, **12**, 4499–4502.

136 W. Gäde and E. Weiss, $[(\eta^5\text{-}CH_3C_5H_4)Mn(CO)_2Hg]_4$, a Compound with an Mn_4Hg_4 Eight-Membered Ring and Additional Hg-Hg Bonds, *Angew. Chem., Int. Ed. Engl.*, 1981, **20**, 803–804.

137 V. G. Albano, C. Castellari, C. Femoni, M. C. Iapalucci, G. Longoni, M. Monari and S. Zacchini, Synthesis, Chemical Characterization, and Molecular Structure of $Au_8\{Fe(CO)_4\}_4(dppe)_2$ and $Au_6Cu_2\{Fe(CO)_4\}_4(dppe)_2$, *J. Cluster Sci.*, 2001, **12**, 75–87.

138 V. G. Albano, M. C. Iapalucci, G. Longoni, M. Monari, A. Paselli and S. Zacchini, Synthesis, Chemical Characterization, and Molecular Structures of $Ag_8Fe_4(CO)_{16}(dppm)_2$ and $Ag_4Au_4Fe_4(CO)_{16}(dppe)_2$, *Organometallcis*, 1998, **17**, 4438–4443.

139 R. Della Pergola, L. Garlaschelli, M. C. Malatesta, C. Manassero and M. Manassero, A Traditional Synthetic Method, and a New Structural Motif, for Molybdenum-Gold Clusters: Synthesis and Solid-State Structure of $Au_8\{Mo(CO)_5\}_4(PPh_3)_4$, *Inorg. Chem.*, 2006, **45**, 8465–8467.

140 B. Berti, M. Bortoluzzi, C. Cesari, C. Femoni, M. C. Iapalucci, L. Soleri and S. Zacchini, Synthesis, Structural Characterization, and DFT Investigations of $[M_xM'_{5-x}Fe_4(CO)_{16}]^{3-}$ (M, M′ = Cu, Ag, Au; M ≠ M′) 2-D Molecular Alloy Clusters, *Inorg. Chem.*, 2020, **59**, 15936–15952.

141 C. Femoni, M. C. Iapalucci, S. Ruggieri and S. Zacchini, From Mononuclear Complexes to Molecular Nanoparticles: The Buildup of Atomically Precise Heterometallic Rhodium Carbonyl Nanoclusters, *Acc. Chem. Res.*, 2018, **51**, 2748–2755.

142 G. Longoni, M. Manassero and M. Sansoni, Synthesis and characterization of new iron-palladium and iron-platinum carbonyl anionic clusters, *J. Am. Chem. Soc.*, 1980, **102**, 3242–3244.

143 J. W. A. van der Velden, J. J. Bour, W. P. Bosman and J. H. Noordik, Reactions of Cationic Gold Clusters with Lewis Bases. Preparation and X-ray Structure Investigation of $[Au_8(PPh_3)_7](NO_3)_2{\cdot}2CH_2Cl_2$ and $Au_6(PPh_3)_4[Co(CO)_4]_2$, *Inorg. Chem.*, 1983, **22**, 1913–1918.

144 Y.-B. Lee and W.-T. Wong, Synthesis and characterization of high-nuclearity osmium-silver mixed-metal clusters, *Chem. Commun.*, 2007, 3924–3926.

145 J. Zhang and L. F. Dahl, First-known high-nuclearity silver-nickel carbonyl cluster: nanosized $[Ag_{16}Ni_{24}(CO)_{40}]^{4-}$ possessing a new 40-atom cubic T_d closed-packed metal-core geometry, *J. Chem. Soc., Dalton Trans.*, 2002, 1269–1274.

146 B. Berti, I. Ciabatti, C. Femoni, M. C. Iapalucci and S. Zacchini, Cluster Core Isomerism Induced by Crystal Packing Effects in the $[HCo_{15}Pd_9C_3(CO)_{38}]^{2-}$ Molecular Nanocluster, *ACS Omega*, 2018, **3**, 13239–13250.

147 I. Ciabatti, C. Femoni, M. Gaboardi, M. C. Iapalucci, G. Longoni, D. Pontiroli, M. Riccò and S. Zacchini, Structural rearrangements induced by acid-base reactions in metal carbonyl clusters: the case of $[H_{3-n}Co_{15}Pd_9C_3(CO)_{38}]^{n-}$ (n = 0-3), *Dalton Trans.*, 2014, **43**, 4388–4399.

148 I. Ciabatti, F. Fabrizi de Biani, C. Femoni, M. C. Iapalucci, G. Longoni and S. Zacchini, Metal Segregation in Bimetallic Co-Pd Carbide Carbonyl Clusters: Synthesis, Structure, Reactivity and Electrochemistry of $[H_{6-n}Co_{20}Pd_{16}C_4(CO)_{48}]^{n-}$ (n = 3-6), *ChemPlusChem*, 2013, **78**, 1456–1465.

149 C. Femoni, M. C. Iapalucci, G. Longoni, C. Tiozzo and S. Zacchini, An Organometallic Approach to Gold Nanoparticles: Synthesis and X-Ray Structure of CO-Protected $Au_{21}Fe_{10}$, $Au_{22}Fe_{12}$, $Au_{28}Fe_{14}$, and $Au_{34}Fe_{14}$ Clusters, *Angew. Chem., Int. Ed.*, 2008, **47**, 6666–6669.

150 B. Berti, M. Bortoluzzi, C. Cesari, C. Femoni, M. C. Iapalucci, R. Mazzoni, F. Vacca and S. Zacchini, Thermal Growth of Au-Fe Heterometallic Carbonyl Clusters Containing N-Heterocyclic Carbene and Phosphine Ligands, *Inorg. Chem.*, 2020, **59**, 2228–2240.

151 K. Konishi, M. Iwasaki and Y. Shichibu, Phosphine-Ligated Gold Clusters with Core + *exo* Geometries: Unique Properties and Interactions at the Ligand-Cluster Interface, *Acc. Chem. Res.*, 2018, **51**, 3125–3133.

152 M. R. Narouz, K. M. Osten, P. J. Unsworth, R. W. Y. Man, K. Salorinne, S. Takano, R. Tomihara, S. Kaappa, S. Malola, C.-T. Dinh, J. D. Padmos, K. Ayoo, P. J. Garrett, M. Nambo, J. H. Horton, E. H. Sargent, H. Häkkinen, T. Tsukuda and C. M. Crudden, N-heterocyclic carbine-functionalized magic-number gold nanoclusters, *Nat. Commun.*, 2019, **11**, 419–425.

153 S. Zhou, W. Pei, Q. Du and J. Zhao, Foreign atom encapsulated Au_{12} golden cages for catalysis of CO oxidation, *Phys. Chem. Chem. Phys.*, 2019, **21**, 10587–10593.

154 M. R. Radzhabov and N. P. Mankad, Activation of robust bonds by carbonyl complexes of Mn, Fe and Co, *Chem. Commun.*, 2023, **59**, 11932–11946.

155 T. Kawawaki, Y. Mitomi, N. Nishi, R. Kurosaki, K. Oiwa, T. Tanaka, H. Hirase, S. Miyajima, Y. Niihori, D. J. Osborn, T. Koitaya, G. F. Metha, T. Yokoyama, K. Iida and Y. Negishi, Pt_{17} nanocluster electrocatalysts: preparation and origin of high oxygen reduction reaction activity, *Nanoscale*, 2023, **15**, 7272–7279.

156 C. Schmitt, N. Da Roit, M. Neumaier, C. B. Maliakkal, D. Wang, T. Henrich, C. Kübel, M. Kappes and S. Behrens, Continuous flow synthesis of atom-precise platinum clusters, *Nanoscale Adv.*, 2024, **6**, 2459–2468.

157 Y. Negishi, Metal-nanocluster science and technology: my personal history and outlook, *Phys. Chem. Chem. Phys.*, 2022, **24**, 7569–7594.

158 F. Forti, C. Cesari, M. Bortoluzzi, C. Femoni, M. C. Iapalucci and S. Zacchini, Heterometallic Ru-Ir clusters as catalyst precursors for hydrogenation and hydrogen transfer reactions, *New J. Chem.*, 2023, **47**, 19289–19303.

159 G. Bussoli, A. Boccalini, M. Bortoluzzi, C. Cesari, M. C. Iapalucci, T. Funaioli, G. Scorzoni, S. Zacchini, S. Ruggieri and C. Femoni, Atomically precise rhodium-indium carbonyl nanoclusters: synthesis, characterization, crystal structure and electron-sponge features, *Nanoscale*, 2024, **16**, 17852–17867.

160 C. Femoni, M. C. Iapalucci, G. Longoni, J. Wolowska, S. Zacchini, P. Zanello, S. Fedi, M. Riccò, D. Pontiroli and M. Mazzani, Magnetic Behavior of Odd- and Even-Electron Metal Carbonyl Clusters: The Case Study of $[Co_8Pt_4C_2(CO)_{24}]^{n-}$ (n = 1, 2) Carbide Cluster, *J. Am. Chem. Soc.*, 2010, **132**, 2919–2927.

161 E. I. Muetterties, T. N. Rhodin, E. Band, C. F. Brucker and W. R. Pretzer, Clusters and Surfaces, *Chem. Rev.*, 1979, **79**, 91–137.

162 E. I. Muetterties and J. Stein, Mechanistic Features of Catalytic Carbon Monoxide Hydrogenation Reactions, *Chem. Rev.*, 1979, **79**, 479–490.

163 C. R. Cobb, R. K. Ngo, E. J. Dick, V. M. Lynch and M. J. Rose, Multi-phosphine-chelated iron-carbide clusters *via* redox-promoted ligand exchange on an inert hexa-iron-carbide carbonyl cluster, $[Fe_6(\mu_6C)(\mu_2\text{-}CO)_4(CO)_{12}]^{2-}$, *Chem. Sci.*, 2024, **15**, 11455–11471.

164 C. Joseph, C. R. Cobb and M. J. Rose, Single-Step Sulfur Insertion into Iron Carbide Carbonyl Clusters: Unlocking the Synthetic Door to FeMoco Analogues, *Angew. Chem., Int. Ed.*, 2021, **60**, 3433–3437.

165 L. K. Batchelor, B. Berti, C. Cesari, I. Ciabatti, P. J. Dyson, C. Femoni, M. C. Iapalucci, M. Mor, S. Ruggieri and S. Zacchini, Water soluble derivatives of platinum carbonyl Chini clusters: synthesis, molecular structures and cytotoxicity of $[Pt_{12}(CO)_{20}(PTA)_4]^{2-}$ and $[Pt_{15}(CO)_{25}(PTA)_5]^{2-}$, *Dalton Trans.*, 2018, **47**, 4467–4477.

166 X. Wang and M. Zhu, Structural Isomerism in Atomically Precise Nanoclusters, *Chem. Mater.*, 2021, **33**, 39–62.

167 J.-H. Huang, X.-Y. Dong, Y.-J. Wang and S.-Q. Zang, Generation and manipulation of chiroptical activities in coinage-metal clusters, *Coord. Chem. Rev.*, 2022, **470**, 214729.

168 C. Cesari, C. Femoni, F. Forti, M. C. Iapalucci, G. Scorzoni and S. Zacchini, Isomerism in Molecular Metal Carbonyl Clusters, *Eur. J. Inorg. Chem.*, 2024, **27**, e202400220.

169 C. Cesari, I. Ciabatti, C. Femoni, M. C. Iapalucci, F. Mancini and S. Zacchini, Heteroleptic Chini-Type Platinum Clusters: Synthesis and Characterization of Bis-Phosphine Derivatives of $[Pt_{3n}(CO)_{6n}]^{2-}$ (n = 2–4), *Inorg. Chem.*, 2017, **56**, 1655–1668.

170 M.-C. Hsu, R. Y. Lin, T.-Y. Sun, Y.-X. Huang, M.-S. Li, Y.-H. Li, H.-L. Chen and M. Shieh, Inorganic-organic hybrid Cu-dipyridyl semiconducting polymers based on the redox-active cluster $[SFe_3(CO)_9]^{2-}$: filling the gap in iron carbonyl chalcogenide polymers, *Dalton Trans.*, 2024, **53m**, 7303–7314.

171 X. Zhao, W.-J. Chen, Q.-M. Liang, S.-K. Chen, J. Xun, B.-J. Geng, H.-F. Su and Y. Yang, Ag^+-Induced Assembly of Pt Clusters for Photocatalytic Hydrogen Production, *Inorg. Chem.*, 2024, **63**, 17672–17680.

172 K. L. Kollmannsberger, Poonam, C. Cesari, R. Khare, T. Kratky, M. Boniface, O. Tomanec, J. Michalička, E. Mosconi, A. Gagliardi, S. Günther, W. Kaiser, T. Lunkenbein, S. Zacchini, J. Warnan and R. A. Fischer, Mechanistic Insights into ZIF-8 Encapsulation of Atom-Precise Pt(M) Carbonyl Clusters, *Chem. Mater.*, 2023, **35**, 5475–5486.

173 P. M. Schneider, K. L. Kollmannsberger, C. Cesari, R. Khare, M. Boniface, B. Roldán Cuenya, T. Lunkenbein, M. Elsner, S. Zacchini, A. S. Bandarenka, J. Warnan and R. A. Fischer, Engineering ORR Electrocatalysts from Co_8Pt_4 Carbonyl Clusters via ZIF-8 Templating, *ChemElectroChem*, 2024, **11**, e202300476.

174 D. Bonincontro, A. Lolli, A. Storione, A. Gasparotto, B. Berti, S. Zacchini, N. Dimitratos and S. Albonetti, Pt and Pt/Sn carbonyl clusters as precursors for the synthesis of supported metal catalysts for the base-free oxidation of HMF, *Appl. Catal., A*, 2019, **588**, 117279.

175 F. Bertolotti, D. Moscheni, A. Migliori, S. Zacchini, A. Cervellino, A. Guagliardi and N. Masciocchi, A total scattering Debye function analysis study of faulted Pt nanocrystals embedded in a porous matrix, *Acta Crystallogr.*, 2016, **A72**, 632–644.

176 I. Robinson, S. Zacchini, L. D. Tung, S. Maenosono and N. T. K. Thanh, Synthesis and Characterization of Magnetic Nanoalloys from Bimetallic Carbonyl Clusters, *Chem. Mater.*, 2009, **21**, 3021–3026.

177 D. A. Serban, P. Greco, S. Melinte, A. Vlad, C. A. Dutu, S. Zacchini, M. C. Iapalucci, F. Biscarini and M. Cavallini, Towards All-Organic Field-Effect Transistors by Additive Soft Lithography, *Small*, 2009, **10**, 1117–1122.

178 P. Greco, M. Cavallini, P. Stoliar, S. D. Quiroga, S. Dutta, S. Zacchini, M. C. Iapalucci, V. Morandi, S. Milita, P. G. Merli and F. Biscarini, Conductive Sub-micrometric Wires of Platinum-Carbonyl Clusters Fabricated by Soft-Lithography, *J. Am. Chem. Soc.*, 2008, **130**, 1177–1182.